Evolution of the Iberian Massif as deduced from its crustal thickness and geometry of a mid-crustal (Conrad) discontinuity

Puy Ayarza[1], José Ramón Martínez Catalán[1], Ana Martínez García[2], Juan Alcalde[2], Juvenal Andrés[1,2], José Fernando Simancas[3], Immaculada Palomeras[1], David Martí[2,4], Irene DeFelipe[2], Chris Juhlin[5], Ramón Carbonell[2]

1. Geology Department, Salamanca University. Pza de la Merced, s/n. Salamanca 37008. Spain
2. Geosciences Barcelona, CSIC. Lluis Solé i Sabaris, s/n. Barcelona 08028. Spain
3. Geodynamics Department, Granada University. Av/ de la Fuente Nueva, s/n. Granada 18071. Spain
4. Lithica SCCL. Avinguda Farners 16, Santa Coloma de Farners, Girona 17430. Spain
5. Department of Earth Sciences, Uppsala University. Villavägen 16, Uppsala, 75236. Sweden

Corresponding author: Puy Ayarza (puy@usal.es)

Abstract

Normal incidence seismic data provide the best images of the crust and lithosphere. When properly designed and continuous, these sections greatly contribute to understanding the geometry of orogens and, together with surface geology, to unravel their evolution. In this paper we present the most complete transect, to date, of the Iberian Massif, the westernmost exposure of the European Variscides. Despite the heterogeneity of the dataset, acquired during the last 30 years, the images resulting from reprocessing with a homogeneous workflow allow us to clearly define the crustal thickness and its internal architecture. The Iberian Massif crust, formed by the amalgamation of continental pieces belonging to Gondwana and Laurussia (Avalonian margin) is well structured in upper and lower crust. A conspicuous mid-crustal discontinuity is clearly defined by the top of the reflective lower crust and by the asymptotic geometry of reflections that merge into it, suggesting that it has often acted as a detachment. The geometry and position of this discontinuity can give us insights on the evolution of the orogen, i.e. of the magnitude of compression and the effects and extent of later Variscan gravitational collapse. Also, the limited thickness of the lower crust in central and NW Iberia might have constrained the response of the Iberian microplate to Alpine shortening. This discontinuity, featuring a Vp increase, is here observed as an orogen-scale boundary with characteristics compatible with those of the worldwide debated, Conrad discontinuity.

Keywords: Iberian Massif, vertical incidence seismic data, mid-crustal detachment, Conrad discontinuity, geodynamic evolution

Glossary:

CIA: Central Iberian Arc
CIZ: Central Iberian Zone
CU: Central Unit
CZ: Cantabrian Zone
DB: Duero Basin
GTMZ: Galicia Tras-os-Montes Zone
IAA: Ibero-Armorican Arc

ICS: Iberian Central System
NI: Normal Incidence
OMA: Ossa-Morena Zone
SPZ: South Portuguese Zone
TB: Tajo Basin
WA: Wide Angle
WALZ: West Asturian-Leonese Zone

1. Introduction

In the last 35 years, controlled source seismic data have greatly contributed to the understanding of the European Variscides. National research programs like DEKORP (Bortfeld, 1985; DEKORP Research Group, 1987; Franke et al., 1990; Oncken, 1998), BIRPS and ECORS (BIRPS and ECORS, 1986) have sampled this orogen providing a detailed picture of its lithospheric architecture. In the Iberian Massif, normal incidence (NI) seismic reflection profiles often acquired with coincident wide angle (WA) reflection/refraction seismic data have allowed scientists to depict its crustal structure, infer its P and S waves velocity distribution, place constraints on its geodynamic evolution, visualize the accommodation pattern of shortening at different crustal levels and, sometimes, deduce the effect of Alpine reactivation on this Paleozoic orogen.

In this regard, seismic datasets acquired in the Iberian Massif (DeFelipe et al., 2020) from the programs ESCIN (Ayarza et al., 1998, 2004; Pérez-Estaún et al., 1991; Pulgar et al., 1996), IBERSEIS (Flecha et al., 2009; Palomeras et al., 2009; Simancas et al., 2003), ALCUDIA (e.g., Ehsan et al., 2014, 2015; Martínez Poyatos et al., 2012) and CIMDEF (Andrés et al., 2019) have helped so far to identify several outstanding features such as, i) clear differences in the intensity and geometry of reflectivity at upper and lower crustal levels, ii) contrasting deformation patterns deduced from the good correlation between reflectivity and upper crustal structures as, regardless of the many factors that trigger the concentration of deformation along narrow thrust zones (Butler and Mazzoli, 2006), the latter often follow lithological boundaries in the Iberian Massif (e.g., Alonso, 1987), thus being candidates to appear as outstanding reflections in NI seismic sections, and iii) a very reflective and sometimes thick lower crust, even in areas where the upper crust is weakly deformed. In order to explain these features, decoupling of the upper and lower crust has been invoked along large parts of the sampled area (Simancas et al., 2013). The existence of a mid-crustal detachment has been addressed by these authors as the reason why different shortening mechanisms exist at different crustal levels. However, coupled crustal deformation has been inferred for NW Iberia, where large crustal thickening took place. Also, no inference has been made on how this detachment acted during later Alpine deformation in the central and northern Iberian Massif.

In this paper, we present a new composite seismic section of the Iberian Massif that integrates results of two new datasets: CIMDEF and ALCUDIA WA. The former fill the gaps of areas previously unexplored, like Central Iberia, altogether providing an almost complete transect. In addition, we include the N-S ESCIN-2 seismic profile and new time-migrated sections of all

datasets, some of them, as yet, unmigrated (e.g., ESCIN-1). Although the detailed interpretation of the upper crustal reflectivity and its correlation with the surface geology does not significantly change, we revisit the deep reflectivity and redefine the extension and implications of a mid-crustal discontinuity that, in our view, exists below the entire Iberian Massif, affecting the two continents involved in the Variscan Orogeny and certainly playing a critical role in the decoupling between upper and lower crustal deformation. Finally, we infer the geometry and nature of this feature, discuss its tectonic significance and its role during the younger Alpine Orogeny, and relate it with the long-debated (e.g., Finlayson et al., 1984; Litak and Brown, 1989; Wever, 1989; Xiaobo and Tae Kyung, 2010) Conrad discontinuity (Conrad, 1925) of the classic continental seismology.

2. Geological setting

The Iberian Massif represents the westernmost outcrop of the European Variscides, exposing an almost complete section of this Paleozoic orogen. It is divided into six zones (Fig. 1; Arenas et al., 1988; Farias et al., 1987; Julivert et al., 1972) that from N to S and E to W are: Cantabrian (CZ), West Asturian-Leonese (WALZ), Galicia-Trás-os-Montes (GTMZ), Central Iberian (CIZ), Ossa-Morena (OMZ) and South Portuguese (SPZ). The CZ and the SPZ represent the external zones whereas the rest represent the hinterland. The CZ, WALZ and CIZ belong to the northern margin of the Paleozoic Gondwana. The GTMZ represents the remnants of a large nappe stack formed by pieces of the outermost margin of the Gondwana margin, i.e., a pulled-apart peri-Gondwanan terrane and oceanic units derived from the oceanic realm separating them. They were emplaced above the autochthonous CIZ in NW Iberia and are preserved as a large klippen at the core of late Variscan synforms (Martínez Catalán et al., 1997, 2007; Ries and Shackleton, 1971). Its rootless suture (ophiolitic units) is thought to represent a branch of the Rheic oceanic realm (Martínez Catalán et al., 1997). The OMZ has been interpreted as a continental fragment that rifted and probably drifted away from Gondwana (Matte, 2001; Robardet, 2002), docking back later to the CIZ giving rise to a suture and thus representing another peri-Gondwanan terrane (Azor et al., 1994; Gómez-Pugnaire et al., 2003; Simancas et al., 2001). Finally, the SPZ is thought to be separated from the OMZ by the Rheic Ocean suture (Simancas et al., 2003) which was later overprinted by early Carboniferous extension accompanied by mafic intrusions (Azor et al., 2008) and by transpression (Pérez-Cáceres et al., 2015). In this context, the basement of the SPZ represents a fragment of Avalonia (Braid et al., 2011, 2012; Pereira et al., 2014; Rodrigues et al., 2015), and its affinity with the Rheno-Hercynian Zone in Germany (Franke, 2000; Franke et al., 1990) further supports this correlation.

From a tectonic point of view, the Iberian Massif shows evidence of pre-Variscan activity. The Cadomian Neoproterozoic event is characterized by continental arc magmatism, deformation and metamorphism (Bandrés et al., 2004; Dallmeyer and Quesada, 1992; Ochsner, 1993). It developed above a previous non-outcropping continental crust, and formed the basement above which the Ediacaran and Paleozoic sedimentation took place, favored by Ediacaran-Cambrian and Cambro-Ordovician rifting which developed a wide continental platform (Linnemann et al., 2008; Sánchez-García et al., 2008, 2010). However, most of the outcropping tectonic features are the result of the Devonian and Carboniferous collision between Gondwana, some peri-Gondwanan terranes and the Avalonian border of Laurentia, which resulted in the Variscan Orogen (Matte, 2001). The deformation associated to the latter was

diachronous along the Iberian Massif. Next, we describe this part of the European Variscides, from N to S (in present coordinates), together with its most important tectonic and stratigraphic features.

The CZ (Fig. 1) is an external zone located at the core of the Ibero-Armorican Arc (IAA; Dias and Ribeiro, 1995; Lotze, 1929; Matte and Ribeiro, 1975; Stille, 1924). It is a thin-skinned thrust and fold belt with a transport direction towards the foreland in the E, and overprinted by the oroclinal folding giving rise to the IAA (Alonso et al., 2009; Pérez-Estaún et al., 1988). Stratigraphically, it is characterized by a Precambrian sequence, outcropping at its western part and overlain by a Paleozoic stratigraphic succession that ranges from the Cambrian to a well-developed Carboniferous: pre-orogenic up to early Carboniferous, and syn-orogenic in the Upper Carboniferous (Sánchez de Posada et al., 1990; Truyols et al., 1990). Scarce tholeiitic and alkaline magmatism is related to Cambro-Ordovician rifting (Corretgé and Suárez, 1990). No regional metamorphism accompanied deformation, indicating shallow crustal conditions. In this area, deformation began at ~325-320 Ma, in the Late Mississippian (Dallmeyer et al., 1997), and the emplacement of nappes that characterize the deformation and the formation of folds within each sequence took place between the Westphalian B and the Stephanian (313-300 Ma), in the Upper Carboniferous (Pérez-Estaún et al., 1988). An extensional episode related to the end of the orogeny led to the formation of Permian Basins (Martínez García, 1981). Later on, extension related to the opening of the Bay of Biscay triggered the development of deep Cretaceous basins (Quintana et al., 2015; Rat, 1988). Alpine tectonics uplifted the Pyrenean-Cantabrian range from the end of the Late Cretaceous to the Miocene (DeFelipe et al., 2019; Teixell et al., 2018 and references therein) reactivating Variscan thrusts and Mesozoic normal faults (Gallastegui et al., 2016).

The WALZ lies to the W of the CZ (Fig. 1). Stratigraphically it consists of a Neoproterozoic terrigenous sequence unconformably overlain by a Paleozoic platform succession that ranges from the Cambrian to the Lower Devonian(Pérez-Estaún et al., 1990), much thicker than that of the CZ. These sediments were actively deformed along three compressional (C1, C2, and C3) and two extensional (E1 and E2) phases during the Variscan Orogeny (Martínez Catalán et al., 2014). Large E vergent folds witness the C1 related compression (360-340 Ma). Those were later affected by E vergence thrusts resulting from ongoing shortening (345-325 Ma). Crustal thickening followed by thermal relaxation led to syn-orogenic extension during E1 (330-315 Ma). A last compressional episode (C3, 315-305 Ma) produced upright folds associated with wrench shear zones while simultaneous extension (E2, 315-300 Ma) continued, characterizing the latest stages of the orogeny in this area. Crustal melting triggered by compression and thickening led to extension and to the intrusion of granitoids in the western part of the WALZ. Thermal models show that the crust could have started to melt within 30 Ma after the onset of crustal thickening, which is then constrained by the ages of Variscan granitoids (Alcock et al., 2009).

The CIZ is the largest of the Iberian Massif zones. Curvature of magnetic anomalies and that of early (C1) Variscan folds depict the Central Iberian Arc (CIA; Martínez Catalán, 2011a, 2011b), partly explaining the width of this internal zone (Fig. 1). The stratigraphic sequence differs from N to S: Ordovician felsic metavolcanic, subvolcanic and intrusives (Diez-Montes et al., 2010) represent the most ancient lithologies outcropping in the N, defining the 'Ollo de Sapo'

domain whereas to the S, Upper-Proterozoic-Lower Cambrian metasediments outcrop (Díez Balda et al., 1995), defining the 'Schist-Greywacke Complex' domain. The pre-orogenic sedimentary sequence continues to the Devonian, followed by a syn-orogenic Carboniferous sequence (Martínez Catalán et al., 2004; Robardet, 2002). This area represents a relatively stable Gondwana margin characterized by the Early Ordovician extension that opened the Rheic Ocean and allowed intrusion of essentially felsic magmas (Díez Montes et al., 2010). The deformation phases described for the WALZ affected most of the CIZ although C1, C2 and E1 are somewhat older, according to the propagation of deformation from the hinterland. Slight differences in the importance of phases can also be found to the center and S (Martínez Catalán et al., 2019), allowing the CIZ to be divided in two zones. In the NW, intense recumbent C1 folds and important C2 thrusts related to the emplacement of the GTMZ occur. Outcropping rocks show epi- to catazonal metamorphism and ductile detachments. Gneiss domes of both E1 and E2 extensional phases exist, evidencing significant crustal thinning, and Variscan granitoids are abundant. To the S, C1 folds are upright, C2 deformation is limited to the southernmost part, and upright C3 folds are the most important structures (Martínez Catalán et al., 2012; Martínez Poyatos, 2002). Metamorphism is generally weak and the amount of granitoids decreases, except in the Iberian Central System (ICS). Here extension postdates C3 upright folding and thus, it is considered E2. Alpine tectonics in the CIZ reactivated previous Variscan fractures and triggered the development of the Iberian Central System (ICS) mountain belt (de Vicente et al., 1996), allowing the products of syn- and post-E2 crustal melting to outcrop in large areas.

The GTMZ is represented by five klippen that are the remnants of the emplacement of a thick nappe stack on top of the CIZ. This includes, from bottom to top, a relatively distal part of the northern Gondwana margin (Parautochthon), the outermost edge of that margin (Lower Allochthon), a few oceanic units of Cambro-Ordovician and Lower Devonian age (Middle Allochthon) and a peri-Gondwanan terrane with magmatic evidences of Cambro-Ordovician rifting and a continental arc setting (Upper Allochthon). Several units show high-P metamorphism reflecting subduction of the ocean represented by the Middle Allochthon and involving also the Upper and Lower ones (Arenas et al., 2007; Gómez Barreiro et al., 2007; Martínez Catalán et al., 2007; Sánchez Martínez et al., 2007). Ongoing subduction during most of the Devonian (400-365 Ma) built an accretionary wedge that was subsequently emplaced on top of the CIZ during the early Carboniferous (C1-C2 events, 360-340 Ma).

The boundary between the CIZ and the OMZ (the Badajoz Córdoba Shear Zone) has been largely interpreted as a suture (Gómez-Pugnaire et al., 2003; Simancas et al., 2001), although no true oceanic units have been identified. It includes amphibolites of oceanic affinity from the early Paleozoic, as well as eclogite relics. In SW Iberia, outcropping lithologies range from the Upper Precambrian to the Upper Carboniferous, with an angular unconformity at the Lower Carboniferous. In the OMZ, the Serie Negra (Black Series) is a thick Neoproterozoic sequence that includes graphitic quartzites and schists and underwent Cadomian arc-related magmatism and regional metamorphism (Dallmeyer and Quesada, 1992; Ochsner, 1993; Quesada and Dallmeyer, 1994). The pre-orogenic Paleozoic sequence is rather complete and was deposited at the peri-Gondwanan platform, as for the CIZ, although differences in the faunal content and in the Paleozoic facies, generally more pelitic in the OMZ, point to a more distal position (Robardet, 2002; Robardet and Gutiérrez Marco, 1990). Ediacaran-Cambrian and Cambro-

Ordovician magmatism reflects two rifting events. The latter is the most important one, it includes alkaline magmatism and is related to the opening of the Rheic Ocean (García Casquero et al., 1985; Ochsner, 1993; Sánchez-García et al., 2008, 2010). The first deformation event, of Devonian age, formed overturned and recumbent folds and thrust faults with SW vergence (Expósito et al., 2002, 2003). Syn-orogenic, early Carboniferous basins developed in an extensional context and are related to calc-alkaline volcanism and magmatism (Casquet et al., 2001). These deposits unconformably overlay the early folds and thrusts. Later, deformation continued with middle and upper Carboniferous sinistral transpression and associated upright NW-SE folds.

A salient seismic reflector, the Iberseis Reflective Body (IRB, Carbonell et al., 2004; Simancas et al., 2003) seems to be the result of a mantle-derived intrusion located along a mid-crustal detachment at around 350-340 Ma. It was emplaced in the context of early Carboniferous extension in the SW of the Iberian Massif, while the hinterland to the NW was undergoing the first stages of compression (C1-C2). Magmatic activity in the SW triggered a high-T/low-P metamorphism that, otherwise, has a low grade elsewhere in the OMZ (Díaz Azpiroz et al., 2006; Pereira et al., 2009).

The boundary between the OMZ and the SPZ has been long understood as a suture on the basis of geometric assumptions (e.g., Carvalho, 1972). Later evidences have reinforced this point of view suggesting that the above mentioned boundary represents the remnants of the Rheic Ocean, although Carboniferous transtension and transpression have largely obliterated it (Pérez-Cáceres et al., 2015 and references therein). The SPZ is a Variscan foredeep basin strongly deformed by thin-skinned thrust tectonics, and is usually correlated with the Rhenohercynian Zone of Kossmat (1927) in the Bohemian Massif. It features wide outcrops of low or very low grade Devonian phyllites, quartzites and sandstones overlain by a lower Carboniferous (Early Mississippian) volcano-sedimentary sequence topped by middle and upper Carboniferous flysch (Oliveira, 1990). From a tectonic point of view, it is characterized by Carboniferous S vergent thrusts and folds, the latter featuring axial traces oblique to the northern boundary of the zone, evidencing transpression (Simancas et al., 2003 and references therein). Deformation propagated towards the S along the lower and upper Carboniferous (Oliveira, 1990).

Although the start of the Variscan collision seems to have been frontal or maybe right-lateral in most of Europe (Shelley and Bossière, 2000), surface geology and interpretation of seismic data evidences the existence of relevant left lateral transpression and oblique-slip syn-metamorphic shear zones in the OMZ, SPZ and their boundaries (Pérez-Cáceres et al., 2016; Simancas et al., 2003 and references therein). In the OMZ, folds and thrusts witnessing Devonian and early Carboniferous compression are oblique to the OMZ/SPZ boundary, indicating a transpressional setting. These features are disrupted by later Mississippian transtensional tectonics (Expósito et al., 2002) that gave way to the intrusion of the Beja-Acebuches mafic and ultramafic rocks (Azor et al., 2008). Convergence resumed soon after, leading to the emplacement of the Beja–Acebuches unit onto the OMZ (Pérez-Cáceres et al., 2015). Inside the OMZ, Devonian and Carboniferous left lateral deformation accounts for ~400 km, higher than perpendicular shortening. Likewise, inside the SPZ, left-lateral displacement is

estimated to reach 90 km whereas the orthogonal one amounts ~60 km (Pérez-Cáceres et al., 2016).

3. Geophysical setting: Existing datasets, their reprocessing and a brief description

3.1. Seismic datasets sampling the Iberian Massif

Since the early 1990s, the Iberian Massif has been sampled by different controlled source seismic experiments (DeFelipe et al., 2020): the ESCIN (1991-1992), IBERSEIS (2000 and 2003), and ALCUDIA (2007-2012) experiments acquired normal incidence (NI) and coincident wide-angle (WA) data. The latest project, carried out with the target of understanding the structure and effect of the Alpine reactivation across the central part of the Iberian Massif, is the CIMDEF experiment (2017-2019). It recorded densely spaced controlled source WA reflection and natural source (earthquakes and noise) seismic data. However, the acquisition of coincident NI data along this transect has not currently been planned, regardless of its potential quality and relevance, due to the relatively high costs of this kind of experiment.

From N to S, and from E to W, the ESCIN project sampled the northern part of the Iberian Massif (Fig. 1). Profile ESCIN-1 (1991) is an onshore E-W line crossing the CZ from its eastern, most external part to its boundary with the WALZ to the W; Profile ESCIN-2 (1991) is an onshore N-S profile crossing the most external and eastern part of the CZ and reaching the northern end of the Duero Basin (DB) to the S, which represents the Cantabrian Mountains foreland basin. The ESCIN-3 (1992) profiles sampled the WALZ and the CIZ along the northern Iberia shelf. Although it consists of three parts (ESCIN-3.1, 3.2 and 3.3) only the easternmost ones (3.2 and 3.3.) are relevant for the study of the Variscan crust and thus, included here. ESCIN-3.3 crossed the entire WALZ to its western boundary with the CIZ, which in this area was surveyed by the ESCIN-3.2. Geographically, the latter also sampled the allochthonous GTMZ. But as this is an offshore profile, it shows no evidences of the presence of the GTMZ, and most of the imaged crust corresponds to that of its relative autochthon, the CIZ.

A significant geographical and methodological gap exists between the ESCIN profiles to the N and the location of the CIMDEF experiment (Fig. 1). The latter crosses central Iberia from the N part of the CIZ, then samples the DB down to the ICS, and goes on S across the Tajo Basin (TB) till it reaches again the CIZ metasediments to the S of the ICS.

In the southern part of the Iberian Massif, the onshore ALCUDIA seismic line (NI and WA), striking NE-SW, was acquired across the CIZ, going from the S of the ICS to the boundary with the OMZ. Finally, the NE-SW IBERSEIS dataset (NI and WA) is also an onshore profile that partially overlaps the same structures as the SW end of the ALCUDIA line although with some 50 km of offset to the W. This seismic line samples the southern part of the CIZ, the OMZ and the SPZ.

Altogether these seismic profiles account for a ~1500 km long seismic transect geared to understand the crustal and, in places, lithospheric structure of the Iberian Massif and to constrain its evolution.

3.2. Processing of datasets

The data used in this work have been acquired at different times, have different characteristics (onshore and offshore) and accordingly exhibit very heterogeneous quality. Table 1 shows the acquisition parameters of all these datasets. The most outstanding differences are: i) the quality and characteristics of the offshore (ESCIN-3) vs the onshore data, ii) the difference between the low fold (30) ESCIN-1, ESCIN-2 and ESCIN-3 data acquired with an explosive source and airguns respectively and the high fold (>60) IBERSEIS and ALCUDIA datasets, which used Vibroseis trucks as source of energy, and iii) the fact that the CIMDEF dataset lacks NI data and only provides lower resolution noise and earthquake data, since WA profiles are, as yet, unpublished. Thus, reprocessing all NI data was mandatory, at least at stack and post-stack level. Figure 2 shows the processing flow followed to homogenize the display of datasets while preserving the true amplitude (Martínez García, 2019). The software package used for reprocessing was GLOBE Claritas (www.globeclaritas.com/) and the most important steps were related to frequency filtering, amplitude weighting and equalization, Kirchhoff time migration and coherency filtering (Fig. 2). In addition, up to 20 multi-trace attribute analysis were tested with the goal to enhance structural and lithological impedance contrasts that allowed to improve the interpretation (Chopra and Alexeev, 2005; Taner and Sheriff, 1977). Although this methodology has been mostly used in sedimentary reservoirs, we have seen that the application of these techniques can enhance the continuity of reflections and help to identify different types of crust, thus easing the interpretation. Some of the boundaries resulting from this attribute analysis (e.g., variance and chaos attribute filters, the former estimating the local variance in the signal and the latter measuring the lack of organization in the reflectivity) are included in the interpretations.

3.3. Description of the seismic sections

The NI datasets included in this paper have already been presented, so the reader will be referred, in every sub-section, to previous publications that include detailed descriptions of pre-stack processing and interpretations. Here we will just focus on those features that are essential to our interpretation.

Geological cross-sections coincident with reprocessed time-migrated sections and their interpretations are presented in figure 3 (ESCIN-1), figure 4 (ESCIN-2), figure 5 (ESCIN-3.3), figure 6 (ESCIN-3.2) figure 7 (ALCUDIA) and figure 8 (IBERSEIS). Migration velocities (Fig. 2) are average crustal values as calculated from coincident or nearby WA models. Depth conversion using migration velocities is also carried out. The description of sections will be done from N to S and from E to W. The CIMDEF dataset will be only described in the discussion (Figs. 9 and 10) as it does not include NI data but is key to understanding the geometry of the mid-crustal discontinuity, its late Variscan reworking and its Alpine reactivation.

3.3.1. Cantabrian Zone (ESCIN-1 section)

The ESCIN-1 section is a ~130 km long, E-W profile crossing the CZ from its most external part to the Narcea Antiform to the W, in the boundary with the hinterland (WALZ, Figs. 1 and 3). It consists of two slightly overlapping parts, 1.1 and 1.2, separated a few kilometers in the N-S direction. The complete ESCIN-1 section migrated at v=5600 m/s (Fig. 2) and its interpretation are presented in figure 3.

This section was first described and interpreted over an unmigrated image by Pérez-Estaún et al. (1994). Later works revisited the interpretation, adding travel-time modeling to help on the understanding of the unmigrated data (Gallastegui et al., 1997). The reader is referred to these papers for further details than those provided here.

In the upper crust, the western part shows W-dipping reflections that represent the Variscan imbrication, through a thrust ramp (t in Fig. 3), of the basement under the Paleozoic succession, indicating the proximity of the hinterland (WALZ). In fact, a Neoproterozoic, non-metamorphic sequence outcrops in this area, which is probably underlain by an older crystalline basement. Another prominent W-dipping reflection roughly parallel to t (t') crosscuts subhorizontal ones, defining a pattern that might be providing an out of the plane image of the above mentioned thrust ramp, as this profile lies in the hinge of an arcuate structure, the IAA (Fig. 1b). To the E, the thin skinned tectonics characteristic of this external zone can be interpreted from shallow subhorizontal to W dipping reflections often coincident with outcropping thrusts (ot), as observed in figure 3a. The main one among these, running at around 5 s (TWT), is interpreted as the sole thrust of the thin-skinned orogenic wedge (st). To the W, it gets involved in the crustal ramp (t in Fig. 3) observed at the Narcea Antiform, suggesting that it ends down rooting into the upper part of the lower crust (c). A low reflectivity wedge of undifferentiated basement (b) located between 4-5 and 8.5 s (TWT) exists underneath the easternmost reflections. This may image some pre-Paleozoic basement that is interpreted as upper crust, since the pattern of reflections changes below, suggesting that a significant boundary occurs underneath.

The lower crust shows little reflectivity but seems to be present in the interval between 8.5-14 s (TWT) in the E and between 8.5 and 12 s (TWT) in the W. It features subhorizontal (ir) and W dipping internal reflectivity to the E, the latter (ir') crosscutting the former reflections. These might represent the imprint of Alpine tectonics over a previously deformed/reflective lower crust. To the W, reflectivity seems to be subhorizontal or dipping to the E (ir). Some of the dipping and arcuated reflectivity observed at the edges of section ESCIN-1 (mig in Fig.3 and thereafter) might be related to the migration effects over discontinuous features and caution should be taken when interpreting it.

The Moho along this section (m) is located at nearly 14.5 s TWT (~45 km) in the eastern part, and shallower (12 s TWT, ~36 km) to the W. The crustal thickening observed to the E is probably related to an out of section image of the crustal Alpine root, better observed in profile ESCIN-2, which is described next.

3.3.2. Cantabrian Zone and Duero Basin (ESCIN-2 section)

The ESCIN-2 seismic line is a 65 km long, N-S section that samples the transition between the CZ and the DB (Fig. 1). Even though this profile was geared to study the Alpine structures, it shows how the Variscan features have been inherited and reactivated during the Cenozoic compression between the Iberian Peninsula and the European plate. The section was first presented by Pulgar et al. (1996). Later on, some authors have used this image to constraint the Alpine structure in the North Iberian Margin (e.g., Fernández-Viejo et al., 2000; Gallastegui et al., 2016). However, only Teixell et al. (2018) used a migrated version (4000 m/s) of this section. Here we present the results of a Kirchhoff time migration at v=5600 m/s (Fig. 4).

This seismic line shows, in places, a conspicuous reflectivity that allows a straightforward interpretation. To the S end, the upper crust is characterized by high amplitude horizontal reflectivity representing the DB sedimentary sequence (Fig. 4a). It occupies the interval from 0-3.5 s TWT (s in Fig. 4b, c and d) and appears to be offset by N dipping reflections (t). The latter have been interpreted as S vergent Alpine thrusts affecting the CZ basement and partly the DB sediments. The rest of the crust is less reflective although N dipping reflectivity (ot), also interpreted as imaging Alpine thrusts on the basis of the clearer stack image (Pulgar et al., 1996), crosscuts shallow subhorizontal weak reflections that represent the Paleozoic sedimentary sequence of the CZ (ps).

The lower crust presents higher amplitude reflectivity. In general, a thick band of horizontal reflections located between 7.5 and 12 s (TWT) at the southern part of the profile, bends and dips to the N in the northern part of the line (lc) in response to Alpine compression. Although the stacked section shows that this N dipping reflectivity reaches 14.5 s TWT (Pulgar et al., 1996) the migrated sections (Teixell et al., 2018 and Fig. 4) indicate that these reflections move southward and upward to less than 14 s (TWT), while losing amplitude and coherence. In fact, the geometry of the bottom of the lowermost crust (Moho, m) is deduced on the basis of the geometry of its uppermost part (c), the lower crust internal reflectivity, the stack image (Pulgar et al., 1996), and the amplitude contrasts observed in the attribute analysis (Fig. 4). Furthermore, its depth is solely stablished on the basis of the position of the strongest subhorizontal reflections to the S.

Even though this profile shows the imprint of recent Alpine shortening, no reflections are observed to crosscut the entire crust. In contrast, reflectivity suggests that deformation is decoupled between the upper and lower crust. However, this section is not long and/or reflective enough as to image where the Alpine thrusts (ot) root. Possibly, they merge into the roof of the underthrusted CZ lower crust.

A 1D Vp profile (Fig. 4e) extracted from the coincident WA model (Pulgar et al., 1996) shows a conspicuous velocity increase in the lower crust, at a depth roughly coincident with (c). Depth misfits are due to the effect of the low Vp of the DB sediments not being taken into account in the depth conversion.

3.3.3. West Asturian-Leonese Zone (ESCIN-3.3 section)

The ESCIN-3.3 profile is part of a ~375 km long crooked offshore seismic line consisting in ESCIN-3.1, 3.2 and 3.3. The latter is 137 km long, parallel to the coast and close to it across the WALZ (Fig. 1). It was first presented by Martínez Catalán et al. (1995) and Ayarza et al. (1998, 2004). Later on, its image has been used to constrain the structure of the western North Iberian Margin and that of the transition between the WALZ and the CIZ (Martínez Catalán et al., 2012, 2014). The cross-section presented in figure 5a corresponds to the equivalent onshore transect of this profile.

Reflectivity in the upper crust is characterized by the image of Mesozoic sedimentary basins (s in Fig. 5) related to the extension that led to the opening of the Bay of Biscay. Underneath, W dipping reflections (t) are interpreted as the imprint of the first stages of Variscan compressional deformation in the WALZ (C1 and C2), developing E-vergent thrust faults (Fig.

5a). These affect the pre-Paleozoic basement and root in the upper part (c) of a thick reflective band interpreted as the lower crust (lc) or in a sole thrust (st) that also reaches the lower crust.

The lower crust (lc) is represented by a thick band of subhorizontal reflectivity (8-12 s TWT) that thickens (6-12 s TWT) in the westernmost part of the WALZ (CDP 3000) underneath the Lugo Dome, an extensional structure bounded to the E by the Viveiro normal fault (Fig. 5). Then it thins towards the end of the line, when entering the CIZ, coinciding with an area of E dipping sub-crustal reflections (sc) altogether defining a less clear Moho (m) in this area. The ESCIN-3.3 lower crust seems to feature an internal layer with mantle P-wave velocities when modeled from coincident WA data. Accordingly it was interpreted as consisting of the WALZ lower crust underthrusted by the CZ lower crust (Ayarza et al., 1998). This model would compensate the high shortening observed in the upper crust of the CZ, a thin-skinned belt whose sole thrust roots at the contact with the WALZ. The internal reflectivity of the lower crust shows W dipping reflectors (ir), similar to the ones observed in the upper crust and probably imaging Variscan deformation in the lower crust, either compressional or extensional. They crosscut subhorizontal reflectivity, thus postdating it. A 1D P-wave velocity profile (Fig. 5e) derived from coincident WA data (Ayarza et al., 1998) shows again an important increase in relation to the top of the lower crust (c).

Even though migration (v= 5200 m/s, Fig. 2) over discontinuous reflections blurs the seismic section in the edges (mig in Fig. 5), reflectivity never seems to cross-cut the crust and/or the Moho, indicating that deformation is decoupled at upper and lower crustal level. Subcrustal E dipping reflections (sc) are interpreted as the out-of-the-plane image of the Alpine southward subduction of the Bay of Biscay oceanic crust (Ayarza et al., 1998, 2004), which is out of the scope of this paper.

The boundary between the WALZ and the CIZ is the Viveiro Fault, one of the most striking surface expressions of Late Variscan extensional tectonics, featuring a decompression of ~4kb or 14 km (Reche et al., 1998). To its W, gravitational collapse of a thickened crust and associated crustal extension and melting have played a key role in the orogenic evolution of the CIZ. However, to the E, crustal re-equilibration after C1 and C2 thickening was less important and igneous activity decreases. Even though this fault itself is not identified in the seismic section (Fig. 4), the reflectivity in general varies on both sides of it, featuring a thinner (9 s TWT vs 12 s TWT) and more transparent crust to the W (Fig. 6). In fact the geometry of some reflections (ef) in the boundary between the WALZ and the CIZ, above the thickest lower crust, and the subtractive way the sole thrust (st) merges with the lower crust (st') seem to indicate the effect of extensional tectonics, sometimes reactivating compressional structures (st-st'). Such a reactivation has been described in the base of the main thrust sheet in the WALZ based on structural and metamorphic considerations (Alcock et al., 2009). Conversely, further to the E of the section, reflectivity probably represents the geometry of preserved compressional deformation.

3.3.4. Northern Central Iberian Zone (ESCIN-3.2 section)

The seismic line ESCIN-3.2 is a 97 km long profile, also parallel and close to the coast, that samples the relative autochthon to the GTMZ, i.e. the CIZ (Figs. 1 and 6). It was first described by Álvarez-Marrón et al. (1996) and later by Ayarza et al. (2004). Here it is presented migrated

with a v=5200 m/s (Fig. 2). The cross-section presented in figure 6a corresponds to the equivalent onshore transect of this profile and depicts allochthonous sequences not imaged by the NI data.

This profile shows, in the upper part, a band of high subhorizontal reflectivity that coincides with the location of Mesozoic basins, as in profile ESCIN-3.3 (s in Fig. 6). The rest of the upper crust is not very reflective although a couple of W-dipping reflections (ef) rooting in a thin band of strong reflectivity are observed. These reflections, located in the E of the section from 4.5 s to 8 s TWT, define a sort of duplex, extensional or compressional, but later extended, indicating in any case boudinage and crustal thinning. To the W, the upper crust is very transparent and just a few weak reflections can be observed.

The narrow reflective band at 8-9 s TWT represents the lower crust (lc), and is the most striking feature of this profile. Its 1 s TWT thickness contrasts with that observed in the neighboring ESCIN-3.3 and ESCIN-1 sections, which show a much thicker lower crust (4-5 s TWT). Reflectivity in this band is subhorizontal, although somewhat undulated, while the band itself is slightly inclined to the W. In the E, the Moho (m) is located above 9 s TWT, the shallowest identified so far in the Iberian Massif. Subcrustal E dipping reflections (sc) are again associated to the 3D image of the southward subduction of the oceanic crust of the Bay of Biscay during the Alpine convergence (Ayarza et al., 2004) whereas W dipping features might be related with the CZ lower crust (czlc) underthrusted also underneath the easternmost part of the CIZ.

This profile samples the northern CIZ, where Variscan crustal thickening during C1 and C2, was most important. Consequently, later gravitational collapse triggered extensional tectonics and crustal melting, allowing the intrusion of granites and the development of extensional detachments (with associated metamorphic offsets). The image of line ESCIN-3.2 shows a transparent upper crust to the W suggesting that granites occupy most of it, which is supported by onland geological mapping. Some thrust faults, as those imaged by W-dipping reflections in profile ESCIN-3.3, probably root along this section and are represented by the W-dipping reflections at the base of the upper crust. However, these were later flattened and/or reactivated as extensional detachments by crustal thinning (ef). The narrowness of the highly reflective lower crust here suggests that crustal thinning was largely accommodated at this level, as the upper crust has basically the same thickness as in the ESCIN-3.3 line (up to 6-7 s TWT). In addition, crustal melting might have also affected the top of the lower crust. But even though large parts of the crust were melted, reflectivity exists deep in the upper crust, suggesting that crustal melting was nor pervasive and/or reflectivity is linked to syn- or late-tectonic features.

3.3.5. Southern Central Iberian Zone (ALCUDIA section)

The ALCUDIA seismic profile was first presented by Martínez Poyatos et al. (2012) and reprocessed and further interpreted by Ehsan et al. (2014). It is a more than 220 km long, NE-SW seismic profile sampling the CIZ to the S of the ICS down to the boundary with the OMZ (Fig. 1). Here we presented this section migrated and depth converted using a v=6200 m/s (Figs. 2 and 7).

This profile presents a fairly transparent upper crust when compared to other nearby sections (e.g., IBERSEIS, Fig. 8) although scarce reflectivity exists to the S coinciding with the boundary (suture) between the CIZ and the OMZ, namely, the Central Unit (CU; cu in Fig. 7) and to the presence of vertical folds (vf). Some very transparent zones (g) appear to be in relation with the existence of granitic batholiths. To the N, the intrusion of these granites, associated to the existence of normal faults (ef), is one of the evidences of extensional tectonics affecting the southern part of the CIZ. The rest of the upper crust shows weak and discontinuous reflectivity that responds to the existence of vertical folding affecting lithologies with little impedance contrast. In fact, deformation in the upper crust of this part of the CIZ is weak, with absence of low-dipping structures typical of tangential tectonics.

The lower crust shows a very different image to that of the upper crust. It is a thick band, of up to 6 s TWT (from 4 s to 10 s), of mostly subhorizontal high amplitude reflectivity (lc) that at some points appears to be cut across by N-dipping reflectors (cc). S-dipping internal reflectivity is also identified although more scarce (ir). The lower crust thins in the northern end of the profile, near the ICS, where intrusion of granites and other evidences of crustal re-equilibration suggest that extension played a key role. Accordingly, we suggest that the mechanisms that triggered this lower crustal thinning are related to melting and extension and not with compression, as previously proposed (Ehsan et al., 2014; Martínez Poyatos et al., 2012), and that the N dipping reflectivity observed in the top of the lower crust (c) in that area is the expression of extensional tectonics.

One of the most striking features of this profile is the crocodile-like structure affecting the lower crust at around CMP 10000 (cc and cc'). This structure, most likely related to Variscan shortening, accommodates an important part of the deformation at lower crustal level and evidences that sub-horizontal reflectivity of the lower crust is pre-Variscan, thus raising the question about its precise age and origin. Despite the presence of this feature in the depth continuation of the suture between the CIZ and the OMZ (Fig. 7a), reflectivity does not crosscut the whole crust, suggesting the existence of a detachment in the top of the lower crust. This contrasts with the presence in the upper crust (CU) of retro-eclogites with peak metamorphic conditions of 19 kbar and ~550°C (López Sánchez-Vizcaíno et al., 2003). Finally, the Moho boundary (m) is located at a fairly constant depth (~10 s TWT, i.e. 30-33 km), although the lower crust seems to be preserved and a local crustal imbrication into the mantle is observed underneath the crocodile-like structure. A 1D Vp profile (inset in Fig. 7d) from a coincident WA-data model (Palomeras et al, in press) shows a conspicuous increase of values along more than 15 km starting in the top of the lower crust (c) thus supporting its important thickness.

3.3.6. Central Iberia, Ossa-Morena and South Portuguese Zones (IBERSEIS section)

The IBERSEIS seismic line was first presented by Simancas et al. (2003). A number of later works added information and details to its interpretation (e.g., Carbonell et al., 2004; Schmelzbach et al., 2007, 2008; Simancas et al., 2006). This section crosses the southernmost CIZ, the whole OMZ, and most of the external SPZ (Fig. 1). It samples two major boundaries interpreted as suture zones: that between the CIZ and the OMZ (CU, Azor et al., 1994) and the one bounding the OMZ and the SPZ, which has been largely affected by younger Carboniferous

events (Pérez-Cáceres et al., 2015). The IBERSEIS profile structurally overlaps the ALCUDIA profile along ~30 km, but it is displaced some 50 km to the W. A cross-section along this transect together with its interpretation after migration at v=6000 m/s (Fig. 2) are shown in figure 8.

This section is ~300 km long and features an outstanding reflectivity at upper and lower crustal levels. In the upper crust, a wealth of N dipping reflections (t in Fig. 8) image a S verging thrust and fold belt. In the SPZ, these are most reflective and probably related to normal faults derived from the extension that led to the opening of the Rheic Ocean and later reactivated as thrusts during the Late Carboniferous compression. Some authors link the highest reflective features to the middle Carboniferous volcano-sedimentary complex (Schmelzbach et al., 2008), which might have used these fractures as a conduit, thus enhancing reflectivity. In the OMZ, N dipping reflections probably image Variscan thrust faults (ot) as some coincide with such mapped structures. Their lesser reflectivity might indicate the lack of involvement in the thrusts of lithologies that increase the impedance contrast.

Upper crustal reflectivity in both, the ZOM and SPZ, does not cross to the lower crust, rooting at a mid-crustal level that, in the SPZ is transparent and does not have any particular expression itself but does coincide with the top of the lower crust (c). However, in the OMZ, a reflective layer exists at this depth (irb): it has been defined as the IBERSEIS reflective body (IRB, Simancas et al., 2003), a 140 km long, high velocity conductive feature (Palomeras et al., 2009) that is supposed to represent an early Carboniferous mantle-derived intrusion. Its origin has been related to mantle plume activity that thinned the lithosphere and extracted mantle-derived melts from the ascending astenosphere (Carbonell et al., 2004). Its surface expression are intraorogenic transtensional features (Rubio Pascual et al., 2013; Simancas et al., 2006). Alternatively, Pin et al. (2008) have suggested, based on geochemical constraints, a tectonic scenario of slab break-off for this feature. Internal reflectivity along the IRB is mostly subhorizontal, probably due to the effect of the intrusion along a subhorizontal detachment, and evidences little imprint from Variscan deformation. The body is slightly inclined to the S, at odds with the detachment being the sole thrust of the OMZ upper crustal imbricates. Perhaps it was, but its inclination changed during subsequent deformation, as later suggested.

The lower crust shows slightly different patterns in the CIZ and OMZ on one side and the SPZ on the other. In the southernmost part of the CIZ and northern OMZ, N and S dipping reflections define a wedge (cc) that might be the western continuation of the crocodile-like structure observed in the ALCUDIA seismic line in an equivalent structural position (cc in Fig. 7). In this section, the limited crustal imbrication into the mantle identified in the ALCUDIA line (cc' in Fig. 7) is not observed, perhaps because it only occurs further to the N or E. This structure may be the reason why the IRB is shallower at this point, indicating that the latter is older than the crocodile compressional feature. The rest of the lower crust shows S dipping and sub-horizontal (lc) reflectivity that does not exhibit clear crosscutting relationships, thus hindering their interpretation. However, near the boundary with the SPZ, this reflectivity seems to be affected by N dipping features (ir) overprinting them. In the SPZ, the lower crust shows a more homogeneous image, with subhorizontal reflectivity (lc) that is often cut across by longer scale S dipping features (lct) that postdate them. The latter probably represent fractures that firstly accommodated the extension linked to the opening of the Rheic Ocean

and were then reactivated as thrusts during the late Carboniferous compression and collision of the SPZ basement with the OMZ. The most conspicuous of these reflections (lct') cuts the IRB in its southern part and seems to offset the lower crustal upper boundary between the SPZ and the OMZ. Two 1D Vp profiles derived from coincident WA-data (Palomeras et al., 2009) and shown as insets in figure 8d indicate a velocity increase starting at the top of lower crust (c) and along the IRB.

Even though the lower crust in the OMZ and SPZ shows dipping features, none of them crosses to the upper crust, thus rooting at a mid-crustal level as does the upper crustal reflectivity. This implies again the existence of a discontinuity (c) in the mid-crust.

Despite of crossing two suture zones and imaging part of a crocodile-like structure, the IBERSEIS profile shows a fairly flat Moho (m) located at ~10 s TWT, the same apparent depth as in the ALCUDIA line (30-33 km). Its signature is very clear underneath the SPZ and a bit blurry below the IRB.

4. Discussion

Simancas et al. (2013) already undertook an integrated interpretation of most of the seismic sections presented here focusing on, i) the accommodation of orogenic shortening at crustal scale, (ii) the relationships between convergence, crustal thickening and collisional granitic magmatism, and (iii) the development of the Iberian Variscan oroclines. In this paper the same sections are presented, but they have been reprocessed at stack level and time migrated using a Kirchhoff algorithm. In addition, two extra sections that image the alleged mid-crustal discontinuity after the Alpine reactivation are taken into account. The first one is the N-S ESCIN-2 NI dataset (Fig. 4), in the CZ, where this discontinuity has remained untouched during late Variscan evolution but was reactivated during the Alpine Orogeny. The second one results from the CIMDEF experiment, carried out in the CIZ across the ICS, where the mid-crustal discontinuity has probably been affected by crustal melting during the Late-Variscan extension and by later Alpine reactivation. The latter sections somehow fill the gap existing in Simancas et al. (2013).

Figures 3 to 8 represent an effort to show a homogeneous seismic image of the Iberian Massif crust that eased its integrated interpretation. Next, we discuss the main observed features, their implications and how they contribute to the understanding of the structure and evolution of the Iberian Massif, adding constraints to the origin of the elevation of the central Iberian Peninsula. Figure 9 presents a simplified sketch of the crustal layers observed in the Iberian Massif. Figure 10 shows a compendium of the position of the mid-crustal discontinuity and the Moho depth (in TWT) along the entire Iberian Massif as deduced from seismic NI data together with a map of the entire Iberian Peninsula Moho depth (Palomeras et al., 2017) that includes the position of the seismic profiles for comparison. We will refer to these figures along most of the discussion.

A particular feature of the SW Iberian Massif is the great importance of out-of-section, mainly left-lateral shear zones associated to its suture boundaries. They displaced central and northern Iberia to the NW with respect to southern Iberia (Simancas et al., 2013). The seismic

sections do not provide constraints about this movement, as it is perpendicular to their layout. Thus, interpretations in these areas must be taken with caution.

4.1. The upper crust in the Iberian Massif: a depth image of outcropping geology

Most of the seismic sections display a moderate to thick upper crust (4 to 8 s TWT, Fig. 9), with very variable reflectivity. Reflections coincide with outcropping Variscan structures and thus, a link has been stablished. As such, N dipping reflectivity in the SPZ and the OMZ is related to S vergent folds and thrust faults mapped in the surface. W dipping reflections in the CZ are related to mapped thin-skinned thrusts. The same type of reflectivity observed in the WALZ, reaching deeper levels in the crust and rooting in the lower crust, has been addressed as evidence of thick-skinned thrust tectonics, which in the hinterland affects the pre-Paleozoic basement. Particularly interesting is the upper crustal SPZ seismic image in contrast with that of the CZ, both representing external zones. While in the latter thrusts are observed to root in a shallow sole detachment, in the former one reflections/thrusts root in the lower crust. This feature will be discussed in the next section.

Only a few seismic profiles feature a transparent upper crust. Lack of reflectivity has been addressed to low fold data (ESCIN-1 and ESCIN-2, Figs 3 and 4), and most importantly to the existence of a re-equilibrated upper crust having recorded large amounts of partial melting, as shown by voluminous outcropping granitoids (ESCIN-3.2 and N of ALCUDIA, Figs. 6 and 7). The existence of vertical folds affecting little reflective monotonous lithologies also results in a fairly transparent upper crust in most of the ALCUDIA section (Fig. 7).

None of the upper crustal reflections observed and interpreted in the presented Iberian Massif NI seismic sections seems to cut across the whole crust, always rooting in a sole thrust (parts of ESCIN-1 and ESCIN-3.3, Figs. 3 and 5) or in the lower crust (the rest of them).

4.2. The lower crust in the Iberian Massif: accommodation of shortening, extension and its nature

The Iberian Massif dataset presented here shows a very coherent image of the lower crust. Its reflectivity is high and usually subhorizontal. However, cross cutting relationships with later features of opposite dips evidence a multi-phase origin for this reflectivity.

The SPZ, OMZ, WALZ, CZ and the southern CIZ show that this part of the crust is also thick (4 to 6 s TWT). However, in NW Iberia and the northern part of the ALCUDIA section (Figs. 1, 6 and 7), the few existing NI profiles indicate that the in the northern CIZ, the lower crust is much thinner (1 to 2 s TWT) and irregular (ESCIN-3.2, Figs. 6 and 9). This thin lower crust has been observed in the area characterized by outcropping syn-collisional granitoids (zone II of Simancas et al., 2013). These witness the onset of crustal re-equilibration processes triggered by gravitational collapse, extension and crustal melting during the Late Carboniferous. The straightforward conclusion is to attribute the architecture of this lower crust to late Variscan orogenic extension, which features at the surface high metamorphic offsets (chlorite to sillimanite zone, Díez Balda et al., 1995) and melting, implying that crustal thinning has been mostly accommodated by its lowermost part.

Nevertheless, a gap of crustal-scale NI data exists in most of the northern CIZ. The CIMDEF noise autocorrelation profiles (Figs. 1 and 9 and) show a thick (~5 s TWT) lower crust in most of this area, which essentially corresponds to the CIZ (Andrés et al., 2019, 2020). This is in conflict with the NI sections ESCIN-3.2 and northernmost ALCUDIA, where the highly reflective lower crust is less than half as thick. However, granitoids are probably scarce in the Variscan basement hidden under the DB, which can then present a thick lower crust. But in and near the ICS, a rather continuous internal reflection in the lower crust could be interpreted as its top part (Figs. 9 and 10), thus indicating that crustal thinning and melting, observed in the surface, has also affected the lower crust (Andrés et al., 2020).

Extension in the northern CIZ occurred simultaneously with shortening in the SW Iberian Massif. According to Simancas et al. (2013) this suggests that the tectonic stresses would be dominantly compressional, still induced by ongoing collision. In fact, gravitational instabilities in a thickened crust should mostly be affecting the upper crust. In this context, theoretical models (Royden, 1996; Seyferth and Henk, 2004) indicate that beneath the areas of extension in the upper crust, shortening may prevail in the lower crust. This mechanism is an efficient way for syn-convergent exhumation of deep rocks.

Indeed, from a regional tectonic perspective, compression was active till the end of the Variscan orogeny, and at times, clearly simultaneous with extension (C3 and E2 overlapped in the interval 315-305 Ma; Martínez Catalán et al., 2014). But it is clear that extension affected the lower crust, as it appears thinned in areas of transparent, extended molten crust (ESCIN-3.2 and ALCUDIA sections, Figs. 6 and 7). However, the irregular pattern observed in the ESCIN-3.2 lower crust might indicate the existence of folds in this re-equilibrated layer, witnessing the simultaneity of extension and compression even at lower crustal level (Fig. 6). In addition, we cannot rule out that these undulations represent boudinage (i.e. extension) or Alpine folding, although we consider the latter less likely.

In the ALCUDIA section, the imaged part of the CIZ underwent only moderate upper crustal shortening (Martínez Poyatos et al., 2012). According to Simancas et al. (2013), the thick laminated lower crust, representing pre-Pennsylvanian (most probably pre-Variscan) ductile deformation, appears deformed in two sectors near both ends of the profile, concentrating shortening in discrete structures that compensate the upper crustal deformation. The first of them is the very conspicuous crocodile-like structure observed in the southern end, and also imaged in the northern part of the IBERSEIS line (Fig. 9b). This structure mimics localized crustal indentation of the OMZ into the CIZ, producing a local underthrusting of the latter to the S that is still (partly?) preserved. Indentation generated tectonic inversion of the Los Pedroches early Carboniferous basin (Simancas et al., 2013) and bending of the overlying upper crust, as seen by the uplift of the IRB, both of which predate the imbrication. The Los Pedroches batholith intruded above at 314-304 Ma in an extensional setting (Carracedo et al., 2009), postdating the age of the wedge as no further deformation affected the batholith. Indeed, the crocodile-like feature must represent early Carboniferous Variscan compressional deformation and must account for part of the shortening observed at upper crustal level.

However, to the NE of this section, a ramp-and-flat geometry has been interpreted as a major lower crustal thrust (Martínez Poyatos et al., 2012; Simancas et al., 2013) that helps to

compensate upper and lower crustal shortening. However, the highly reflective lower crust is not repeated in the hanging wall to the structure, so that a subtractive character is a reasonable alternative. As stated above, the thin lower crust to the N of the ramp seems to be clear evidence of lower crustal thinning (Fig. 9b), supported by the fact that it underlies an area of upper crustal extension, the Toledo gneiss dome, characterized by normal faulting and pervasive partial melting (Barbero, 1995; Hernández Enrile, 1991). Regardless of how much shortening that area accommodated during crustal thickening and even though the observed ramp could be a former thrust fault reactivated during later extension, the present image of the lower crust does not suggests compensation of upper crustal shortening. In fact, the lower crust in the ALCUDIA section is anomalously thick elsewhere (up to 6 s TWT, 18 km) suggesting the possibility of ductile thickening previous to the extension that triggered thinning at its northern part.

In the IBERSEIS profile, lower crustal dominant reflectivity is also subhorizontal but disrupted by N and S dipping features (Fig. 9b). Whereas in the OMZ these features usually dip to the N, as do the upper crustal reflections representing Variscan thrusts, in the SPZ they surprisingly mirror the upper crustal Variscan thrusts, dipping to the S. Furthermore, one of these features, placed close to the boundary with the OMZ, affects almost the entire lower crust.

Orogenic orthogonal shortening in the OMZ upper crust has been estimated in 120 km (~57%) and in the SPZ around 80 km (~45%) or even less (Pérez-Cáceres et al., 2016). According to Simancas et al. (2013), the crocodile structure and a not observed associated northward subduction of the OMZ might account for this shortening in the OMZ. Similarly, in the SPZ, the lower crustal imbricated structures represent only ~ 20 km of shortening so that according to these authors, detached lower crustal subduction along the OMZ/SPZ might have accommodated the other 60 km.

In this regard, we suggest that the present day SPZ crustal image represents its decoupled early Carboniferous extension and later compression. This evolution would have erased any evidences of previous (pre-Carboniferous) subduction, and forced the SPZ to thin during extension. i.e., the lower crust had to decrease its thickness ductilely, perhaps first in a more or less distributed way and later through localized shear zones (brittle or not depending on the depth) as it became shallower. However, the upper crust could have preserved most of its original thickness, as the developing basins associated to extension would have been constantly fed by sediments and igneous extrusions and intrusions (like the IRB in the OMZ). Later compression would have folded and thrusted the upper crust, and also thickened the lower crust. A few lower crustal normal shear zones might have developed during extension and then be reactivated as ductile thrusts during compression. Those are today observed as S dipping reflections that disrupt the subhorizontal previous reflectivity in the lower crust and mirror thrusts in the upper crust. Accordingly, distributed ductile deformation and thrusting might have thickened the lower crust back to its original (or simply stable) thickness in the SPZ and elsewhere, something that cannot be measured but would need to be accounted for when comparing shortening at upper and lower crustal level. The resulting seismic image of the SPZ would then be that of an extended and then inverted margin, with mirroring reflectors in the upper and lower crust merging in a mid-crustal discontinuity and providing a seismic image different to that of a typical foreland thrust and fold belt (e.g., CZ; Fig. 3). This evolution differs

from that of a hyperextended magma-rich margin as stretching of the upper and lower crust is not coupled and faults do not cut across the crust and penetrate down into the mantle. In any case, the S dipping lower crustal reflections, active during the Late Carboniferous, postdate the sub horizontal reflectivity of the lower crust. It is worth mentioning here that the SPZ seismic image is identical to that of the Rhenohercynian Massif in Germany (Franke et al., 1990; Oncken, 1998) suggesting a similar evolution.

The discussion above shows that the lower crust in the Iberian Massif is thick, except when it is affected by late orogenic extension. The mechanisms that produced lower crustal thickening are probably related to compressional deformation, mostly ductile. Continental underthrusting of the CZ underneath the WALZ (Ayarza et al., 1998, 2004) and part of the CIZ (Fig. 6, 9 and 10), indentation of the OMZ in the CIZ (Figs. 9 and 10) and Variscan thrust-like structures probably played an important role. In addition, the latter help to constrain the age of the subhorizontal reflectivity. Frequent disruption of subhorizontal lower crustal lamination by Variscan (late Carboniferous) dipping features indicates that the lamination developed prior to Variscan compressional deformation. What this lamination represents is still an open question.

Many vertical incidence seismic reflection profiles worldwide have shown reflective lower crusts (e.g., Meissner et al., 2006; Wever, 1989). Lower crust seismic lamination has been often related to late orogenic extensional events (Meissner, 1989). In the Iberian Massif, surface geology shows that late orogenic extension affects the upper crust, mainly in areas of large previous thickening. But in contrast to the latter author's models, important thinning of the lower crust takes place in those areas (ESCIN-3.2 and northern ALCUDIA, Figs. 6, 7 and 9). Certainly, lower crustal lamination might come from underplating eased by extension in magma rich margins (Klemperer et al., 1986). But also, ductile deformation is a very likely source of lower crustal lamination. Dipping events observed in the lower crust crosscutting a strong banded reflectivity represent the latest orogeny-related shortening, which will be further flattened and horizontalized in the next orogeny. Continuous superposition of deformational events at lower crustal level managed to decrease the dip of structural/lithological markers and define a subhorizontal fabric. These deformation mechanisms can generate structures with a strongly defined anisotropy, which result in a strongly laminated lower crustal fabric (Carbonell and Smithson, 1991; Okaya et al., 2004). Accordingly, a laminated lower crust may represent an overly reworked lower crust that has been ductilely deformed over several orogenies. Opposite to the model by Meissner (1989), such a horizontal reflectivity is observed along the Iberian Massif in areas where late orogenic extension is absent or weak: the SPZ (Avalonia), the OMZ (peri-Gondwana), the not extended CIZ, the WALZ and the CZ (Gondwana). Thus, we suggest that strong lamination in the deep crust is probably a global characteristic of reworked lower crusts not affected by late orogenic extension in the latest orogeny.

4.3. The Moho and crustal thickness in the Iberian Massif

The crust-mantle boundary, i.e., the Moho, is basically flat in the Iberian Massif except where affected by the Alpine tectonics (Fig. 10). This is rather surprising as the lower crust seems to be quite well preserved, suggesting that the Moho geometry has been flattened out through slow, not invasive, readjustments.

Flat Mohos imply the existence of either isostatic and/or thermal, late to post-orogenic processes that have managed to eliminate crustal roots (Cook, 2002). NW Iberia was affected by late Carboniferous extension that heated and reworked the CIZ, possibly without significant mantle involvement (Alcock et al., 2009, 2011), but producing crustal thinning (Palomeras et al., 2017: see Moho depth map in Fig. 10). Thick and thermally mature crusts might experience lateral flow of its low-viscosity deeper part that contributed to reduce crustal roots (Seyferth and Henk, 2004). This process might have partly occurred in the CIZ sampled by the ESCIN-3.2 section (Fig. 6) where an outstanding change in lower crustal thickness and signature exist, manifested by a thinner and very reflective lower crust in contrast to that to the E, in the WALZ (1 vs 3 s TWT) or to the S, in the ALCUDIA profile (1 vs 5-6 s TWT). In the former, the Variscan crust is still thick even though it experienced late-Variscan extension in its western part and the whole area was slightly affected offshore by the extension linked to the opening of the Bay of Biscay. In fact, underthrusting of the CZ lower crust is still preserved in the eastern CIZ (Figs. 6 and 9).

In the SW Iberian Massif, a thick laminated lower crust is still observable while the Moho depth is fairly constant (~10s TWT). Carboniferous-to-Permian isostatic rebound in response to tectonic thickening, erosion and localized Permian thermal readjustments must have contributed to flatten the Moho. However, seismic reflections show that crustal imbrication into the mantle has locally survived post-orogenic Moho resetting. This indicates that isostatic equilibrium has been reached in a long wavelength scale, but that local features can still remain if they are supported by the crustal strength and do not pose an isostatic constraint.

4.4. The (missing) middle crust in the Iberian Massif (and elsewhere?)

One of the highlights of this work is the lack of a seismic layer that can be identified with the middle crust. But, what is the middle crust?

From a metamorphic point of view, the middle crust could be ascribed to the mesozone, which may be correlated to the amphibolite facies, whose temperature ranges between 400-500 and 600-800°C, the precise limits depending on the pressure (Spear, 1993). In addition, the epizone, between 200-250 and 400-500°C and typically represented by the greenschist facies, is also a metamorphic entity which develops during metamorphism under several kilometers of anchi- and no metamorphic rocks. The depths corresponding to these temperature intervals vary with the geothermal gradient. For a Barrowian gradient, typical of a continental crust undergoing collision, the depths for epizone and mesozone can be estimated around 10-20 and 20-30 (± 5) km respectively. Although the boundaries of these metamorphic zones might have a gravity, i.e. density signature, they lack a seismic one. Furthermore, epi-, meso- and catazonal rocks outcrop everywhere in any eroded orogenic belt defining a very complex pattern that contrasts with the simplicity of seismic images. This implies that the metamorphic middle-crust does not need to coincide with a hypothetic seismic middle crust, the former often being part the upper crust in ancient orogens.

Seismic data are sensible to velocity and density contrasts and not to the absolute value of velocity and density. If a sharp contrast exists, a reflection appears, but metamorphic zones usually lack sharp boundaries. So from a seismic point of view, a middle crust should be a crustal level bounded in its upper and lower parts by reflections indicative of the existence of

important impedance contrasts at its top and bottom. In this regard, only the IRB, intruded between the upper and the lower crust (Carbonell et al., 2004; Simancas et al., 2003), and providing conspicuous velocity contrasts (Palomeras et al., 2009, 2011) fulfill that requirement. However, it is most probably an intrusion emplaced at a mid-crustal discontinuity and does not represent the middle crust.

WA reflection seismic data from the northern Iberian Massif have often resulted in multilayered models despite weak evidences of continuous reflectivity at these levels (Ayarza et al., 1998; Fernández-Viejo et al., 1998, 2000; Pedreira et al., 2003). Even though local velocity contrasts capable of providing weak and patchy reflectivity contrasts exist at different crustal depths (e.g., thrust faults and normal detachments may represent lithological boundaries with a noticeable velocity contrast), these are not orogen-scale features but local reflectors. However, many of these reflections have been extrapolated and interpreted as middle crust in seismic WA datasets, despite of being part of upper crust when compared with NI data, i.e., lie above the mid-crustal discontinuity (e.g., Vp increase at ~10 km in Fig. 5e). In this regard, the short wavelength heterogeneities of the crust have been often considered by low resolution WA datasets as laterally continuous features (Levander and Holliger, 1992), something that has led us to wrong models.

According to the above we argue that, in the Iberian Massif, no seismic middle crust can be identified. In the hinterland, reflectors imaging deformation in the upper crust root in the top of the lower crust. Only in ESCIN-1, which depicts the thin-skinned deformation of the CZ, thrust faults root in a sole thrust and one could argue that the basement underneath these shallow reflections represents the middle crust. But in the shallower part, to the E, early Paleozoic and Neoproterozoic sediments occur on both sides of the sole thrust. Also, in the deeper parts, to the W, the previous crystalline basement is probably involved in imbrications affecting the upper crust. Thus, in our opinion, that non-reflective basement represents the seismic upper crust.

In the Iberian Massif, the Paleozoic was deposited unconformably above Neoproterozoic sediments which could be considered as its basement, but these were not metamorphic then. Only in the OMZ, greenschist to amphibolite facies Neoproterozoic represents the Cadomian basement, but it cannot be distinguished from the overlying Paleozoic metasediments in the NI profiles. An even older crystalline basement of felsic composition exists, as indicated by inherited zircons of 830-2000 Ma found in Ediacaran orthogneisses, Lower Ordovician volcanics and Variscan granitoids that resulted from partial melting of such a basement (Fernández-Suárez et al., 1998; Montero et al., 2007; Villaseca et al., 2012). Again, its upper boundary is not imaged on NI profiles. These data also suggest that, in the Iberian Massif, there are no crustal intervals that can be related to a seismic middle crust. Decoupling of reflectivity, i.e. deformation, at a mid-crustal level led us to define just an upper and a lower crust.

4.5. Significance of a mid-crustal discontinuity: the Conrad discontinuity?

Inspection of the Iberian Massif NI seismic dataset leads us to conclude that an orogenic-scale mid-crustal discontinuity exits. This surface does not always provide a clear reflection, as in the SPZ, but it is clearly defined by the geometry of the upper and lower crustal reflections,

asymptotically merging into it. The discontinuity coincides with the top of the lower crust, which is often much more reflective than the upper crust and features a Vp increase. Furthermore, this discontinuity has probably acted as a detachment for Variscan deformation in the hinterland of the orogen and in the SPZ. However, in the CZ, the transition between upper and lower crust is poorly defined, as most of its basement was not affected by Variscan tectonics.

Simancas et al. (2013) already described this discontinuity on the basis of the asymptotic geometry of the SPZ faults towards the middle of the crust. These authors concluded that its depth greatly varies when reaching suture boundaries, where the discontinuity roots. Although we do not observe a subduction zone in the reworked elusive suture between the SPZ and the OMZ (Pérez-Cáceres et al., 2015), and interpret the OMZ/CIZ suture as an indentation between two continental crusts, triggering imbrication into the mantle of the latter (crocodile structure), we agree that this discontinuity would have eased the decoupling of the Iberian crust, allowing subduction of its lower part while the upper part was deformed by folds and thrust faults. In fact, this is clearly observed in the Alpine northward subduction of the Iberian Massif lower crust underneath the CZ (ESCIN-2, Fig. 4) and also, in the Pyrenees, where a detached Iberian lower crust subducts to the N (Teixell et al., 2018). But in the Iberian Massif, the complexity of Variscan tectonics and late-Variscan crustal re-equilibration has mostly removed evidences of a such mechanisms, although a comparable example has been preserved in the NW: the thick lower crust imaged by ESCIN-3.3 is interpreted as underthrusting of the CZ lower crust under that of the WALZ (Ayarza et al., 1998; Martínez Catalán et al., 2003, 2012, 2014) and even reaching the CIZ, as shown in profile ESCIN-3.2.

Some authors have interpreted the Iberian Massif mid crustal discontinuity as the brittle-ductile transition (e.g. Ehsan et al., 2014; Simancas et al., 2013). Indeed, it bounds a lower crust, highly reflective and ductilely deformed from the upper crust. However, Variscan ductile deformation occurs also above the discontinuity in the entire Iberian Massif, with the exception of the CZ. On the other side, if we deal with present deformation mechanisms, it is unlikely that the brittle-ductile transition, which depends on the values of P and T, coincide with the described discontinuity, because, i) it does not necessarily imply an impedance contrast (Litak and Brown, 1989), and ii) according to figure 10, the depth of the discontinuity varies from 4 s TWT (~12 km, ALCUDIA section) to 8 s TWT (~21 km, ESCIN-2 section) which would imply unrealistic variations on P and T in the present crust. Accordingly, a different interpretation must be sought.

The Iberian laminated lower crust is probably very old. Granulites dredged in Mesozoic sediments of the Cantabrian margin have yielded ages of up to 1400 Ma (Capdevila et al., 1980 and references therein). Even older values have been obtained for the Galicia Bank granulites (Gardien et al., 2000), which featured Ar-Ar ages of up to 2500 Ma. These granulites have been deformed ductilely during several orogenies. But rocks lying above the lower crust, whatever their nature, are separated from it by a discontinuity that fosters decoupled deformation between both crustal layers. Accordingly, the observed mid-crustal discontinuity probably represents a rheological boundary that separates rocks that have been deformed differently. This boundary, located at the top of the lower crust, represents a velocity increase as the latter

is probably composed of dense granulites and includes relatively abundant basic rocks, which makes it easily identifiable in NI and WA seismic sections.

The geometry of this discontinuity and its depth, together with that of the Moho (Fig. 10), provide insights of the evolution of the Iberian Massif. Along the SW Iberian Massif, the mid-crustal discontinuity is sub-horizontal and lies at a depth between 4-6 s TWT. In the OMZ, the intrusion of the IRB allows to stablish its depth in the top or the bottom of this feature, but in average, its location would fit the above given values. However, in the center and NW, the position of the discontinuity varies, deepening down to 8 s TWT (Figs. 9 and 10).

The low resolution noise autocorrelation models obtained along the CIMDEF profile show confusing results along the central Iberian Massif. There, the mid-crustal discontinuity might lie at 5-6 s TWT, deepening around the ICS to 8 s TWT as it has been affected by pervasive extension and melting, thus defining a thin lower crust (2 s TWT, ~6 km, Figs. 9 and 10). Accordingly, this feature appears redefined in this area, and now follows the geometry of the ICS batholith. The change in the depth and geometry of this discontinuity and the thinning of the lower crust might have allowed coupled deformation, letting part of the upper crust to the S of the ICS to underthrust it (Andrés et al., 2020). This would foster the 400-500 m topographic change between the N and S foreland basins of this Alpine mountain range (Fig. 9). In fact, Simancas et al. (2013) argues that coupled crustal deformation takes place when a relatively weak lower crust exists something that might well represent the context of the ICS. The resulting geometry of this Alpine reactivation and its topographic imprint is different to that observed to the N, in the CZ, where late orogenic extension and melting does not exist and the mid-crustal discontinuity has been preserved.

On the other hand, the lower crust imaged along the CIMDEF transect presents a conspicuous internal reflection that could also be interpreted as the top of the lower crust (Andrés et al., 2020). If this were the case, the lower crust would be even thinner along the entire section, matching the characteristics observed to the N of the ALCUDIA section and in the ESCIN-3.2 line. In any case, we argue that the mid-crustal discontinuity and the lower crust seen in the CIMDEF profile are both probably reworked by extension but not totally re-equilibrated and thus, its seismic image is confusing to the N and S of the ICS. Moho depth models (Fig. 10) derived from shear wave tomography (Palomeras et al., 2017) indicate that along the CIMDEF profile the crust is thin (except in the Alpine root) but not as much as in NW Iberia, so that lower crustal extension and re-equilibration may have not been as intense as in the GTMZ and CIZ of the NW Iberian Massif.

The most outstanding change in the mid-crustal discontinuity architecture appears in NW Iberia, along the ESCIN-3.2 profile. This section features the thinnest crust (9 s TWT) accompanied by the thinnest lower crust (~1 s TWT). The mid-crustal discontinuity lies at 8 s TWT in contrast to the depth where it appears in the neighbouring ESCIN-3-3 and ESCIN-1 lines (6 and 8 s TWT), suggesting that it has been redefined. Nevertheless, clear reflections root in its upper part indicating that it still acted as a discontinuity/detachment. The depth of this feature in NW Iberia is similar to that of the high amplitude lower crustal internal reflection near the ICS. Accordingly, we suggest that in NW Iberia, gravitational collapse followed by

crustal melting and extension has thinned the crust (Fig. 10), and specially the lower crust, relocating the mid-crustal discontinuity.

NW Iberia was importantly thickened (up to 50-70 km) due to the emplacement of the GTMZ allochtonous complexes. Thermal models by Alcock et al. (2009, 2015) show that as a result, the upper mantle continued increasing its temperature 60-65 Ma after the start of compressional deformation at 360 Ma. This implies large thinning of the mantle lithosphere, from 70 to 25-30 km, due to the ascent of the 1300 °C isotherm. It is not surprising that the lower crust there became highly extended as a consequence of the heat increase, as in the models it reached 800 °C after 45 Ma and 900 °C after 55 Ma (315-305 Ma).

The idea of a mid-crustal velocity discontinuity was put forward in the 1920's (Conrad, 1925). Early analysis of natural source earthquake recordings and later images from controlled source seismic reflection data provided further evidences that supported a clear distinction between upper and lower crust. These evidences led to considering the Conrad discontinuity, a global scale feature present in the continental crust. However, this was later challenged as some results of deep seismic reflection profiling did not show a clear distinction between upper and lower crust (Litak and Brown, 1989).

Mid-crustal discontinuities have, however, been observed often in different types of seismic data worldwide (e.g., Fianco et al., 2019; Hobbs et al., 2004; Melekhova et al., 2019; Oncken, 1998; Ross et al., 2004; Snelson et al., 2013). Important changes in the rheology of the crust have also been reported at those depths (Maggini and Caputo, 2020; Wever, 1989) supporting the idea that a mechanical boundary must exist. Thus, we suggest that, even though it is not observed everywhere (Litak and Brown, 1989), this feature is an orogen-scale, world class continental crustal discontinuity (Artemieva, 2009), often coinciding with the top of the highly laminated lower crust (when there is one). Its existence might determine the way the crust deforms, easing decoupled deformation. Orogenic evolution, i.e. rifting, extension, melting, etc. may modify it or even erase it, thus its existence and geometry might help us to understand the geologic history of continents. In this regard, and coming back to the long-forgotten discussion of the nature of the Conrad discontinuity (Conrad, 1925) and its position on top of the laminated lower crust (Wever, 1989), we suggest that, in the Iberian Massif, the observed mid-crustal feature fulfills the characteristics of this debated discontinuity. Its clear signature and regional extension contributes to unravel its nature and significance.

5. Conclusions

Normal incidence seismic data acquired across the Iberian Massif in the last 30 years have provided an entire section of a well exposed and almost complete part of the European Variscides. Existing gaps in the central part have been recently sampled by passive source seismic recordings (noise and earthquakes) that provide fairly good constraints on the crustal structure.

Results show that crustal thickness varies from ~9 s TWT in late-Variscan extended areas (NW of the Central Iberian Zone), to ~10 s TWT (30-33 km) in the external South Portuguese Zone to ~12 s TWT (36-38 km) in the internal West Asturian-Leonese Zone. Alpine reactivation has managed to further thicken the crust to at least ~14 s TWT (42-45 km) in the external

Cantabrian Zone and to 35-38 km in the Iberian Central System, a Tertiary orogenic belt developed in Central Spain. The top of an often thick (up to 6 s TWT) and very reflective lower crust helps to define a mid-crustal discontinuity across the entire Iberian Massif. This boundary represents a level where reflections from the upper and lower crust merge asymptotically, thus suggesting that it has often acted as a detachment or a decoupling level. Its position and geometry varies mostly in relation to the late Variscan evolution. Accordingly, it is deeper in NW and central Iberia (~8 s TWT), where Variscan crustal thickening was important and gravitational collapse melted and extended the crust, thus defining a very thin lower crust. However, it appears between 4-6 s TWT to the SW, where the crust did not thicken as much and its original structure is better preserved, being later re-equilibrated through slow isostasy and erosion.

This discontinuity exists in all the Iberian Massif tectonic zones, regardless of their Gondwana or Avalonia affinity, thus suggesting it is an orogenic-scale discontinuity. We interpret it as the rheological boundary between an overly ductilely deformed old lower crust and a heterogeneous variably (often also ductilely) deformed upper crust that mostly (but not only) shows evidences of the latest orogenic event. Its geometry, position and extent match the characteristics defined for the long-forgotten Conrad discontinuity. The identification of similar features in normal incidence profiles worldwide supports its inclusion as a major crustal discontinuity.

Acknowledgements

The seismic data was reprocessed using the commercial seismic signal processing software Claritas. Funding for this research was provided by the Junta de Castilla y León (SA065P17), the Spanish Ministry of Science and Innovation (CGL2016-78560-P) and the Generalitat de Catalunya (grant 2017SGR1022). The comments of Prof. R.W.H. Butler and an anonymous reviewer have greatly contributed to improve this manuscript.

References

Alcock, J. E., Martínez Catalán, J. R., Arenas, R. and Díez Montes, A.: Use of thermal modeling to assess the tectono-metamorphic history of the Lugo and Sanabria gneiss domes, Northwest Iberia, Bull. la Soc. Geol. Fr., 180(3), 179–197, doi:10.2113/gssgfbull.180.3.179, 2009.

Alcock, J. E., Martínez Catalán, J. R. and Arenas, R.: One- and two-dimensional models are equally effective in monitoring the crust's thermal response to advection by large-scale thrusting during orogenesis, Comput. Geosci., 37(8), 1205–1207, doi:10.1016/j.cageo.2011.02.012, 2011.

Alcock, J. E., Martínez Catalán, J. R., Rubio Pascual, F. J., Díez Montes, A., Díez Fernández, R., Gómez Barreiro, J., Arenas, R., Dias da Silva, Í. and González Clavijo, E.: 2-D thermal modeling of HT-LP metamorphism in NW and Central Iberia: Implications for Variscan magmatism, rheology of the lithosphere and orogenic evolution, Tectonophysics, 657, 21–37, doi:10.1016/j.tecto.2015.05.022, 2015.

Alonso, J. L.: Sequences of thrusts and displacement transfer in the superposed duplexes of the Esla Nappe Region (cantabrian zone, nw spain), J. Struct. Geol., 9(8), 969–983, doi:10.1016/0191-8141(87)90005-8, 1987.

Alonso, J. L., Marcos, A. and Suárez, A.: Paleogeographic inversion resulting from large out of sequence breaching thrusts: The León Fault (Cantabrian zone, NW Iberia). A new picture of the external Variscan thrust belt in the Ibero-Armorican arc, Geol. Acta, 7(4), 451–473, doi:10.1344/105.000001449, 2009.

Álvarez-Marrón, J., Pérez-Estaún, A., Dañobeitia, J. J., Pulgar, J. A., Martínez Catalán, J. R., Marcos, A., Bastida, F., Ayarza, P., Aller, J., Gallart, A., González-Lodeiro, F., Banda, E., Comas, M. C. and Córdoba, D.: Seismic structure of the northern continental margin of Spain from ESCIN deep seismic profiles, Tectonophysics, 264, 153–174, doi:10.1016/S0040-1951(96)00124-2, 1996.

Andrés, J., Draganov, D., Schimmel, M., Ayarza, P., Palomeras, I., Ruiz, M. and Carbonell, R.: Lithospheric image of the Central Iberian Zone (Iberian Massif) using global-phase seismic interferometry, Solid Earth, 10(6), 1937–1950, doi:10.5194/se-10-1937-2019, 2019.

Andrés, J., Ayarza, P., Schimmel, M., Palomeras, I., Ruiz, M. and Carbonell, R.: What can seismic noise tell us about the Alpine reactivation of the Iberian Massif? An example in the Iberian Central System, Solid Earth, 11(6), 2499–2513, doi:10.5194/se-11-2499-2020, 2020.

Arenas, R., Farias, P., Gallastegui, G., Gil Ibarguchi, I., González Lodeiro, F., Klein, E., Marquínez, J., Martín Parra, L. M., Martínez Catalán, J. R., Ortega, E., de Pablo Maciá, J. G., Peinado, M. and Rodriguez Fernández, L. R.: Características geológicas y significado de los dominios que componen la Zona de Galicia-Trás-os- Montes. Simposio sobre Cinturones Orogénicos, in Simposio sobre Cinturones Orogénicos. II cogreso Geológico de España, pp. 75–84, SGE., 1988.

Arenas, R., Martínez Catalán, J. R., Martínez Sánchez, S., Díaz García, F., Abati, J., Fernández-Suárez, J., Andonaegui, P. and Gómez-Barreiro, J.: Paleozoic ophiolites in the Variscan suture of Galicia (northwest Spain): Distribution, characteristics, and meaning, Mem. Geol. Soc. Am., 200(22), 425–444, doi:10.1130/2007.1200(22), 2007.

Artemieva, I.: Continental Crust, Geophysics and Geochemestry Vol.II -Encyclopedia of Earth and Atmospheric Sciences in the Global Encyclopedia of Life Support Systems, UNESCO., 2009.

Ayarza, P., Martínez Catalán, J. R., Gallart, J., Pulgar, J. A. and Dañobeitia, J. J.: Estudio Sismico de la Corteza Ibérica Norte 3 . 3 : A seismic image of the Variscan crust inthe hinterland of the NW Iberian Massif, Tectonics, 17(2), 171–186, 1998.

Ayarza, P., Martínez Catalán, J. R., Alvarez-Marrón, J., Zeyen, H. and Juhlin, C.: Geophysical constraints on the deep structure of a limited ocean-continent subduction zone at the North Iberian Margin, Tectonics, 23(1), doi:10.1029/2002TC001487, 2004.

Azor, A., Lodeiro, F. G. and Simancas, J. F.: Tectonic evolution of the boundary between the Central Iberian and Ossa-Morena zones (Variscan belt, southwest Spain), Tectonics, 13(1), 45–61, doi:10.1029/93TC02724, 1994.

Azor, A., Rubatto, D., Simancas, J. F., González Lodeiro, F., Martínez Poyatos, D., Martin Parra, L. M. and Matas, J.: Rheic Ocean ophiolitic remnants in southern Iberia questioned by SHRIMP U-Pb zircon ages on the Beja-Acebuches amphibolites, Tectonics, 27(5), 1–11, doi:10.1029/2008TC002306, 2008.

Bandrés, A., Eguíluz, L., Pin, C., Paquette, J. L., Ordóñez, B., Le Fèvre, B., Ortega, L. A. and Gil Ibarguchi, J. I.: The northern Ossa-Morena Cadomian batholith (Iberian Massif): Magmatic arc origin and early evolution, Int. J. Earth Sci., 93(5), 860–885, doi:10.1007/s00531-004-0423-6, 2004.

1085 Barbero, L.: Granulite-facies metamorphism in the Anatectic Complex of Toledo, Spain: late
1086 Hercynian tectonic evolution by crustal extension, J. Geol. Soc. London, 152(2), 365–382,
1087 doi:10.1144/gsjgs.152.2.0365, 1995.

1088 BIRPS, B. I. R. P. S. and ECORS, E. de la C. C. et O. par R. et R. S.: Deep seismic reflection
1089 profiling between England, France and Ireland., J. - Geol. Soc., 143(1), 45–52,
1090 doi:10.1144/gsjgs.143.1.0045, 1986.

1091 Bortfeld, R. K.: First results and preliminary interpretation of deep- reflection seismic
1092 recordings along profile DEKORP 2-South (FRG)., J. Geophys. - Zeitschrift fur Geophys., 57(3),
1093 137–163, 1985.

1094 Braid, J. A., Brendan Murphy, J., Quesada, C. and Mortensen, J.: Tectonic escape of a crustal
1095 fragment during the closure of the Rheic Ocean: U-Pb detrital zircon data from the late
1096 Palaeozoic Pulo do Lobo and South Portuguese zones, Southern Iberia, J. Geol. Soc. London.,
1097 168(2), 383–392, doi:10.1144/0016-76492010-104, 2011.

1098 Braid, J. A., Murphy, J. B., Quesada, C., Bickerton, L. and Mortensen, J. K.: Probing the
1099 composition of unexposed basement, South Portuguese Zone, southern Iberia: Implications for
1100 the connections between the Appalachian and Variscan orogens, Can. J. Earth Sci., 49(4), 591–
1101 613, doi:10.1139/E11-071, 2012.

1102 Butler, R. W. H. and Mazzoli, S.: Styles of continental contraction: A review and introduction,
1103 Spec. Pap. Geol. Soc. Am., 414(414), 1–10, doi:10.1130/2006.2414(01), 2006.

1104 Capdevila, R., Boillot, G., Lepvrier, C., Malod, J. A. and Mascle, G.: Les formations cristallines du
1105 Banc Le Danois (marge nord-ibérique), CR Acad. Sci. Paris, D, 291(January), 317–320 [online]
1106 Available from:
1107 http://scholar.google.com/scholar?hl=en&btnG=Search&q=intitle:Les+formations+cristallines+
1108 du+Banc+Le+Danois+(marge+nord+ibérique)#0, 1980.

1109 Carbonell, R. and Smithson, S. B.: Large-scale anisotropy within the crust in the Basin and
1110 Range province, Geology, 19(July), 698–701, doi:doi:10.1130/0091-7613(1991)019, 1991.

1111 Carbonell, R., Simancas, J. F., Juhlin, C., Pous, J., Pérez-Estaún, A., Gonzalez-Lodeiro, F., Munoz,
1112 G., Heise, W. and Ayarza, P.: Geophysical evidence of a mantle derived intrusion in SW Iberia,
1113 Geophys. Res. Lett., 31(11), 1–4, 2004.

1114 Carracedo, M., Paquette, J. L., Alonso Olazabal, A., Santos Zalduegui, J. F., de García de
1115 Madinabeitia, S., Tiepolo, M. and Gil Ibarguchi, J. I.: U-Pb dating of granodiorite and granite
1116 units of the Los Pedroches batholith. Implications for geodynamic models of the southern
1117 Central Iberian Zone (Iberian Massif), Int. J. Earth Sci., 98(7), 1609–1624, doi:10.1007/s00531-
1118 008-0317-0, 2009.

1119 Carvalho, D.: The metallogenetic consequences of plate tectonics and the upper Paleozoic
1120 evolution of southern Portugal, Estud. Notas e Trab. S.F.M., 20(3–4), 297–320, 1972.

1121 Casquet, C., Galindo, C., Tornos, F., Velasco, F. and Canales, A.: The Aguablanca Cu-Ni ore
1122 deposit (Extremadura, Spain), a case of synorogenic orthomagmatic mineralization: Age and
1123 isotope composition of magmas (Sr, Nd) and ore (S), Ore Geol. Rev., 18(3–4), 237–250,
1124 doi:10.1016/S0169-1368(01)00033-6, 2001.

1125 Chopra, S. and Alexeev, V.: Application of texture attribute analysis to 3D seismic data, Soc.
1126 Explor. Geophys. - 75th SEG Int. Expo. Annu. Meet. SEG 2005, 30(7), 767–770,
1127 doi:10.1190/1.2144439, 2005.

Conrad, V.: Laufzeitkurven des Tauernbens vom 28, Mitt. Erdb. Komm. WIen Akad. Wiss., 59, 1, 1925.

Cook, F. A.: Fine structure of the continental reflection Moho, Bull. Geol. Soc. Am., 114(1), 64–79, doi:10.1130/0016-7606(2002)114<0064:FSOTCR>2.0.CO;2, 2002.

Corretgé, L. G. and Suárez, O.: Cantabrian and Palentian Zones. Igneous Rocks, in Pre-Mesozoic Geology of Iberia, edited by R. D. Dallmeyer and E. Martínez García, pp. 72–79, Springer-Verlag, Berlin., 1990.

Dallmeyer, R. D. and Quesada, C.: Cadomian vs. Variscan evolution of the Ossa-Morena zone (SW Iberia): field and 40Ar/39Ar mineral age constraints, Tectonophysics, 216(3–4), 339–364, doi:10.1016/0040-1951(92)90405-U, 1992.

Dallmeyer, R. D., Martínez Catalán, J. R., Arenas, R., Gil Ibarguchi, J. I., Gutiérrez-Alonso, G., Farias, P., Bastida, F. and Aller, J.: Diachronous Variscan tectonothermal activity in the NW Iberian Massif: Evidence from 40Ar/39Ar dating of regional fabrics, Tectonophysics, 277(4), 307–337, doi:10.1016/S0040-1951(97)00035-8, 1997.

DeFelipe, I., Pedreira, D., Pulgar, J. A., van der Beek, P. A., Bernet, M. and Pik, R.: Unraveling the Mesozoic and Cenozoic Tectonothermal Evolution of the Eastern Basque-Cantabrian Zone–Western Pyrenees by Low-Temperature Thermochronology, Tectonics, 38(9), 3436–3461, doi:10.1029/2019TC005532, 2019.

DeFelipe, I., Alcalde, J., Ivandic, M., Martí, D., Ruiz, M., Marzán, I., Diaz, J., Ayarza, P., Palomeras, I., Fernandez-Turiel, J. L., Molina, C., Bernal, I., Brown, L., Roberts, R. and Carbonell, R.: Reassessing the lithosphere: SeisDARE, an open access seismic data repository, Earth Syst. Sci. Data Discuss., (September), 1–32, doi:10.5194/essd-2020-208, 2020.

DEKORP Research Group: Results of deep reflection seismic profiling in the Oberpfalz (Bavaria), Geophys. J. R. Astron. Soc., 89(1), 353–360, doi:10.1111/j.1365-246X.1987.tb04430.x, 1987.

Dias, R. and Ribeiro, A.: The Ibero-Armorican Arc: A collision effect against an irregular continent?, Tectonophysics, 246(1–3), 113–128, doi:10.1016/0040-1951(94)00253-6, 1995.

Díaz Azpiroz, M., Fernández, C., Castro, A. and El-Biad, M.: Tectonometamorphic evolution of the Aracena metamorphic belt (SW Spain) resulting from ridge-trench interaction during Variscan plate convergence, Tectonics, 25(1), 1–20, doi:10.1029/2004TC001742, 2006.

Diez-Montes, A., Martínez Catalán, J. R. and Bellido Mulas, F.: Role of the Ollo de Sapo massive felsic volcanism of NW Iberia in the Early Ordovician dynamics of northern Gondwana, Gondwana Res., 17(2–3), 363–376, doi:10.1016/j.gr.2009.09.001, 2010.

Díez Balda, M. A., Martínez Catalán, J. R. and Ayarza, P.: Syn-collisional extensional collapse parallel to the orogenic trend in a domain of steep tectonics: the Salamanca Detachment Zone (Central Iberian Zone, Spain), J. Struct. Geol., 17(2), 163–182, doi:10.1016/0191-8141(94)E0042-W, 1995.

Díez Montes, A., Martínez Catalán, J. R. and Bellido Mulas, F.: Role of the Ollo de Sapo massive felsic volcanism of NW Iberia in the Early Ordovician dynamics of northern Gondwana, Gondwana Res., 17(2–3), 363–376, doi:10.1016/j.gr.2009.09.001, 2010.

Ehsan, S. A., Carbonell, R., Ayarza, P., Martí, D., Pérez-Estaún, A., Martínez-Poyatos, D. J., Simancas, J. F., Azor, A. and Mansilla, L.: Crustal deformation styles along the reprocessed deep seismic reflection transect of the Central Iberian Zone (Iberian Peninsula), Tectonophysics, 621,

159–174, doi:10.1016/j.tecto.2014.02.014, 2014.

Ehsan, S. A., Carbonell, R., Ayarza, P., Martí, D., Martínez Poyatos, D., Simancas, J. F., Azor, A., Ayala, C., Torné, M. and Pérez-Estaún, A.: Lithospheric velocity model across the Southern Central Iberian Zone (Variscan Iberian Massif): The ALCUDIA wide-angle seismic reflection transect, Tectonics, 34(3), 535–554, doi:10.1002/2014TC003661, 2015.

Expósito, I., Simancas, J. F. and Lodeiro, F. G.: Estructura de la mitad septentrional de la zona de Ossa-Morena: Deformación en el bloque inferior de un cabalgamiento cortical de evolución compleja: Deformación en el bloque inferior de un cabalgamiento cortical de evolución compleja, Rev. la Soc. Geológica España, 15(1), 3–14, 2002.

Expósito, I., Simancas, J. F., González Lodeiro, F., Bea, F., Montero, P. and Salman, K.: Metamorphic and deformational imprint of Cambrian - Lower Ordovician rifting in the Ossa-Morena Zone (Iberian Massif, Spain), J. Struct. Geol., 25(12), 2077–2087, doi:10.1016/S0191-8141(03)00075-0, 2003.

Farias, P., Gallastegui, G., González Lodeiro, F., Marquinez, J., Martín-Parra, L. M., Martínez Catalán, J. R. and Pablo-Maciá, J. G.: "Aportaciones al conocimiento de la litoestratigrafia y estructura de Galicia Central," Memórias da Fac. Ciências, Univ. do Porto, 1(January 1987), 411–431, 1987.

Fernández-Suárez, J., Gutiérrez-Alonso, G., Jenner, G. A. and Jackson, S. E.: Geochronology and geochemistry of the Pola de Allande granitoids (northern Spain): their bearing on the Cadomian-Avalonian evolution of northwest Iberia, Can. J. Earth Sci., 35(12), 1439–1453, doi:10.1139/cjes-35-12-1439, 1998.

Fernández-Viejo, G., Gallart, J., Pulgar, J. A., Gallastegui, J., Dañobeitia, D. and Córdoba, D.: Crustal transition between continental and oceanico domains along the North Iberian margin from wide angle seismic and gravity data, Geophys. Res. Lett., 25(23), 4249–4252, 1998.

Fernández-Viejo, G., Gallart, J., Pulgar, A., Córdoba, D. and Dañobeitia, J. J.: Seismic signature of Variscan and Alpine tectonics in NW Iberia: Crustal structure of the Cantabrian Mountains and Duero Basin, J. Geophys. Res., 105(1999), 3001–3018, 2000.

Fianco, C. B., França, G. S., Albuquerque, D. F., Vilar, C. da S. and Argollo, R. M.: Using the receiver function for studying earth deep structure in the Southern Borborema Province, J. South Am. Earth Sci., 94(April), 102221, doi:10.1016/j.jsames.2019.102221, 2019.

Finlayson, D. M., Collins, C. D. N. and Lock, J.: P-wave velocity features of the lithosphere under the Eromanga Basin, Eastern Australia, including a prominent MID-crustal (Conrad?) discontinuity, Tectonophysics, 101(3–4), 267–291, doi:10.1016/0040-1951(84)90117-3, 1984.

Flecha, I., Palomeras, I., Carbonell, R., Simancas, J. F., Ayarza, P., Matas, J., González-Lodeiro, F. and Pérez-Estaún, A.: Seismic imaging and modelling of the lithosphere of SW-Iberia, Tectonophysics, 472(1–4), 148–157, doi:10.1016/j.tecto.2008.05.033, 2009.

Franke, W.: The mid-European segment of the Variscides: Tectonostratigraphic units, terrane boundaries and plate tectonic evolution, Geol. Soc. Spec. Publ., 179, 35–56, doi:10.1144/GSL.SP.2000.179.01.05, 2000.

Franke, W., Bortfeld, R. K., Brix, M., Drozdzewski, G., Dürbaum, H. J., Giese, P., Janoth, W., Jödicke, H., Reichert, C., Scherp, A., Schmoll, J., Thomas, R., Thünker, M., Weber, K., Wiesner, M. G. and Wong, H. K.: Crustal structure of the Rhenish Massif: results of deep seismic reflection lines Dekorp 2-North and 2-North-Q, Geol. Rundschau, 79(3), 523–566,

doi:10.1007/BF01879201, 1990.

Gallastegui, J., Pulgar, J. A. and Alvarez-Marrón, J.: 2-D seismic modeling of the Variscan foreland thrust and fold belt crust in NW Spain from ESCIN-1 deep seismic reflection data, Tectonophysics, 269(1–2), 21–32, doi:10.1016/S0040-1951(96)00166-7, 1997.

Gallastegui, J., Pulgar, J. A. and Gallart, J.: Alpine tectonic wedging and crustal delamination in the Cantabrian Mountains (NW Spain), Solid Earth, 7(4), 1043–1057, doi:10.5194/se-7-1043-2016, 2016.

García Casquero, J. L., Boelrijk, N. A. I. M., Chacón, J. and Priem, H. N. A.: Rb-Sr evidence for the presence of Ordovician gsranites in the deformed basement of the Badajoz-Córdoba belt, SW Spain, Geol. Rundschau, 74(2), 379–384, doi:10.1007/BF01824904, 1985.

Gardien, V., Arnaud, N. and Desmurs, L.: Petrology and ar-ar dating of granulites from the galicia bank (spain): African craton relics in western europe, Geodin. Acta, 13(2–3), 103–117, doi:10.1080/09853111.2000.11105367, 2000.

Gómez-Pugnaire, M. T., Azor, A., Fernández-Soler, J. M. and López Sánchez-Vizcaíno, V.: The amphibolites from the Ossa-Morena/Central Iberian Variscan suture (Southwestern Iberian Massif): Geochemistry and tectonic interpretation, Lithos, 68(1–2), 23–42, doi:10.1016/S0024-4937(03)00018-5, 2003.

Gómez Barreiro, J., Martínez Catalán, J. R., Arenas, R., Castiñeiras, P., Abati, J., Díaz García, F. and Wijbrans, J. R.: Tectonic evolution of the upper allochthon of the Órdenes complex (northwestern Iberian Massif): Structural constraints to a polyorogenic peri-Gondwanan terrane, Geol. Soc. Am. Spec. Pap., 423, 315–332, doi:10.1130/2007.2423(15)., 2007.

Hernández Enrile, J. L.: Extensional tectonics of the toledo ductile-brittle shear zone, central Iberian Massif, Tectonophysics, 191(3–4), 311–324, doi:10.1016/0040-1951(91)90064-Y, 1991.

Hobbs, B. E., Ord, A., Regenauer-Lieb, K. and Drummond, B.: Fluid reservoirs in the crust and mechanical coupling between the upper and lower crust, Earth, Planets Sp., 56(12), 1151–1161, doi:10.1186/BF03353334, 2004.

Julivert, M., Fontboté, M., Ribeiero, A. and Conde, L. E.: Mapa tectónico de la Península Ibérica y Baleares Notas Incluye mapa : Unidades estructurales de la Península Ibérica . Escala 1 : 1.000.000., Instituto Geológico y Minero de España., 1972.

Klemperer, S. L., Hauge, T. A., Hauser, E. C., Oliver, J. E. and Potter, C. J.: The Moho in the northern Basin and Range Province, Nevada, along the COCORP 40oN seismic- reflection transect. (USA)., Geol. Soc. Am. Bull., 97(5), 603–618, doi:10.1130/0016-7606(1986)97<603:TMITNB>2.0.CO;2, 1986.

Kossmat, F.: Gliederung des varistischen Gebirgsbaues. Abhandlungen des Sächsischen, in Abhandlungen des Sächsischen Geologuschen Landesamts, edited by A. des S. G. Landesamts, p. 39, Leipzig, Heft 1., 1927.

Levander, A. R. and Holliger, K.: Small-scale heterogeneity and large-scale velocity structure of the continental crust, J. Geophys. Res., 97(B6), 8797–8804, doi:10.1029/92JB00659, 1992.

Linnemann, U., Pereira, M. F., Jeffries, T. E., Drost, K. and Gerdes, A.: The Cadomian Orogeny and the opening of the Rheic Ocean: The diacrony of geotectonic processes constrained by LA-ICP-MS U-Pb zircon dating (Ossa-Morena and Saxo-Thuringian Zones, Iberian and Bohemian Massifs), Tectonophysics, 461(1–4), 21–43, doi:10.1016/j.tecto.2008.05.002, 2008.

Litak, R. K. and Brown, L. D.: A modern perspective on the Conrad Discontinuity, Eos, Trans. Am. Geophys. Union, 70(29), 713–725, doi:10.1029/89EO00223, 1989.

López Sánchez-Vizcaíno, V., Gómez-Pugnaire, M. T., Azor, A. and Fernández-Soler, J. M.: Phase diagram sections applied to amphibolites: A case study from the Ossa-Morena/Central Iberian Variscan suture (Southwestern Iberian Massif), Lithos, 68(1–2), 1–21, doi:10.1016/S0024-4937(03)00017-3, 2003.

Lotze, F.: Stratigraphie und Tektonik des Keltiberischen Grundgebirges (Spanien), Abhandlungen Gesellschaft der Wissenschaften zu Göttingen, Math. (Abh. Ges. Wiss. Göttingen, Math.-Phys.), 14(2), 143–162, 1929.

Maggini, M. and Caputo, R.: Sensitivity analysis for crustal rheological profiles: Examples from the Aegean region, Ann. Geophys., 63(3), 1–29, doi:10.4401/ag-8244, 2020.

Martínez Catalán, J. R.: Are the oroclines of the Variscan belt related to late Variscan strike-slip tectonics?, Terra Nov., 23(4), 241–247, doi:10.1111/j.1365-3121.2011.01005.x, 2011.

Martínez Catalán, J. R.: The Central Iberian arc, an orocline centered in the Iberian Massif and some implications for the Variscan belt, Int. J. Earth Sci., 101(5), 1299–1314, doi:10.1007/s00531-011-0715-6, 2012.

Martínez Catalán, J. R., Ayarza, P., Pulgar, J. A., Pérez-Estaún, A., Gallart, J., Marcos, A., Bastida, F., Álvarez-Marrón, J., González Lodeiro, F., Aller, J., Dañobeitia, J. J., Banda, E., Córdoba, D. and Comas, M. C.: Results from the ESCIN-N3.3 marine deep seismic profile along the Cantabrian continental margin, Rev. Soc. Geol. España, 8(4), 341-354., 1995.

Martínez Catalán, J. R., Arenas, R., Díaz García, F. and Abati, J.: Variscan accretionary complex of northwest Iberia: Terrane correlation succession of tectonothermal events, Geology, 25(12), 1103–1106, doi:10.1130/0091-7613(1997)025<1103:VACONI>2.3.CO;2, 1997.

Martínez Catalán, J. R., Fernández-Suárez, J., Jenner, G. A., Belousova, E. and Díez Montes, A.: Provenance constraints from detrital zircon U–Pb ages in the NW Iberian Massif: implications for Palaeozoic plate configuration and Variscan evolution, J. Geol. Soc. London., 161(3), 463–476, doi:10.1144/0016-764903-054, 2004.

Martínez Catalán, J. R., Arenas, R., Díagarcía, F., González Cuadra, P., Gómez-Barreiro, J., Abati, J., Castiñeiras, P., Fernández-Suárez, J., Sánchez Martínez, S., Andonaegui, P., González Clavijo, E., Díez Montes, A., Rubio Pascual, F. J. and Valle Aguado, B.: Space and time in the tectonic evolution of the northwestern Iberian Massif: Implications for the Variscan belt, Mem. Geol. Soc. Am., 200(21), 403–423, doi:10.1130/2007.1200(21), 2007.

Martínez Catalán, J. R., Álvarez Lobato, F., Pinto, V., Gómez Barreiro, J., Ayarza, P., Villalaín, J. J. and Casas, A.: Gravity and magnetic anomalies in the allochthonous rdenes Complex (Variscan belt, northwest Spain): Assessing its internal structure and thickness, Tectonics, 31(5), 1–18, doi:10.1029/2011TC003093, 2012.

Martínez Catalán, J. R., Rubio Pascual, F. J., Díez Montes, A., Díez Fernández, R., Gómez Barreiro, J., Dias da Silva, Í., González Clavijo, E., Ayarza, P. and Alcock, J. E.: The late Variscan HT/LP metamorphic event in NW and Central Iberia: relationships to crustal thickening, extension, orocline development and crustal evolution, Geol. Soc. London, Spec. Publ., 405(1), 225–247, doi:10.1144/SP405.1, 2014.

Martínez Catalán, J. R., Díez Balda, M. A., Escuder Viruete, J., Villar Alonso, P., Ayarza, P., Gonalez Clavijo, E. and Dïez Montes, A.: Cizallamientos dúctiles de escala regional en la

provincia de Salamanca, in Geo-Guias: Rutas Geológicas por la Península Ibérica, Canarias, Sicilia y Marruecos, edited by M. Diaz Azpiroz, I. Exposito Ramos, S. Llana Fúnez, and B. Bauluz Lázaro, pp. 109–118, Sociedad Geológica de España., 2019.

Martínez García, A.: Seismic characterization and geodynamic significane of the mid-crustal discontinuity across the Variscan Iberia, Universidad de Barcelona., 2019.

Martínez García, E.: El Paleozoico de la Zona Cantabrica Oriental (Noroeste de España), Trab. Geol., 11, 95–127, 1981.

Martínez Poyatos, D., Carbonell, R., Palomeras, I., Simancas, J. F., Ayarza, P., Martí, D., Azor, A., Jabaloy, A., González Cuadra, P., Tejero, R., Martín Parra, L. M., Matas, J., González Lodeiro, F., Pérez-Estaún, A., García Lobón, J. L. and Mansilla, L.: Imaging the crustal structure of the Central Iberian Zone (Variscan Belt): The ALCUDIA deep seismic reflection transect, Tectonics, 31(3), 1–21, doi:10.1029/2011TC002995, 2012.

Martínez Poyatos, D. J.: Estructura del borde meridional de la Zona Centroibérica y su relación con el contacto entre las Zonas Centroibérica y de Ossa-Morena, in Serie Nova Terra, 18, edited by L. X. de Laxe, p. 295, Instituto Universitario de Xeoloxía, A Coruña, Spain., 2002.

Matte, P.: The Variscan collage and orogeny (480–290 Ma) and the tectonic definition of the Armorica microplate: a review - Matte - 2003 - Terra Nova - Wiley Online Library, Terra Nov., 13(1997), 122–128 [online] Available from: http://onlinelibrary.wiley.com/doi/10.1046/j.1365-3121.2001.00327.x/full%5Cnpapers2://publication/uuid/85445613-EAD8-49D7-AE4E-704E3D282C36, 2001.

Matte, P. and Ribeiro, A.: Forme et orientation de l'ellipsoïde de déformation dans la virgation hercynienne de Galice. Relations avec le plissement et hypothèses sur la genèse de l'arc ibéro-armoricain, Comptes Rendus l'Académie des Sci., 280, 2825–2828, 1975.

Meissner, R.: Rupture, creep, lamellae and crocodiles: happenings in the continental crust, Terra Nov., 1(1), 17–28, doi:10.1111/j.1365-3121.1989.tb00321.x, 1989.

Meissner, R., Rabbel, W. and Kern, H.: Seismic lamination and anisotropy of the lower continental crust, Tectonophysics, 416(1–2), 81–99, doi:10.1016/j.tecto.2005.11.013, 2006.

Melekhova, E., Schlaphorst, D., Blundy, J., Kendall, J. M., Connolly, C., McCarthy, A. and Arculus, R.: Lateral variation in crustal structure along the Lesser Antilles arc from petrology of crustal xenoliths and seismic receiver functions, Earth Planet. Sci. Lett., 516, 12–24, doi:10.1016/j.epsl.2019.03.030, 2019.

Montero, P., Bea, F., González-Lodeiro, F., Talavera, C. and Whitehouse, M. J.: Zircon ages of the metavolcanic rocks and metagranites of the Ollo de Sapo Domain in central Spain: Implications for the Neoproterozoic to Early Palaeozoic evolution of Iberia, Geol. Mag., 144(6), 963–976, doi:10.1017/S0016756807003858, 2007.

Ochsner, A.: U-Pb geochronology of the Upper Proterozoic-Lower Paleozoic geodynamic evolution in the Ossa-Morena Zone (SW Iberia): constraints on the timing of the Cadomian orogeny, University of Zurich, Diss. ETH10, 192., 1993.

Okaya, D., Rabbel, W., Beilecke, T. and Hasenclever, J.: P wave material anisotropy of a tectono-metamorphic terrane: An active source seismic experiment at the KTB super-deep drill hole, southeast Germany, Geophys. Res. Lett., 31(24), 1–4, doi:10.1029/2004GL020855, 2004.

Oliveira, J. T.: Part VI: South Portuguese Zone, stratigraphy and synsedimentary tectonism, in

Pre-Mesozoic Geology of Iberia, edited by E. Dallmeyer, R. D., and Martínez García, pp. 334–347, Springer, Berlin, Germany., 1990.

Oncken, O.: Orogenic mass transfer and reflection seismic patterns - Evidence from DEKORP sections across the European variscides (central Germany), Tectonophysics, 286(1–4), 47–61, doi:10.1016/S0040-1951(97)00254-0, 1998.

Palomeras, I., Carbonell, R., Flecha, I., Simancas, J. F., Ayarza, P., Matas, J., Poyatos, D. M., Azor, A., Lodeiro, F. G. and Pérez-Estaún, A.: Nature of the lithosphere across the Variscan orogen of SW Iberia: Dense wide-angle seismic reflection data, J. Geophys. Res. Solid Earth, 114(2), 1–29, 2009.

Palomeras, I., Carbonell, R., Ayarza, P., Martí, D., Brown, D. and Simancas, J. F.: Shear wave modeling and Poisson's ratio in the Variscan Belt of SW Iberia, Geochemistry, Geophys. Geosystems, 12(7), 1–23, doi:10.1029/2011GC003577, 2011.

Palomeras, I., Villaseñor, A., Thurner, S., Levander, A., Gallart, J. and Harnafi, M.: Lithospheric strcuture of Iberia and Morocco using finite-frequency Rayleigh wave tomogrpahy from earthquakes and seismic ambient noise, Geochemistry, Geophys. Geosystems, 1–17, doi:10.1002/2016GC006657, 2017.

Pedreira, D., Pulgar, J. A., Gallart, J. and Díaz, J.: Seismic evidence of Alpine crustal thickening and wedging from the western Pyrenees to the Cantabrian Mountains (north Iberia), J. Geophys. Res., 108(B4), 1–21, doi:10.1029/2001JB001667, 2003.

Pereira, M. F., Chichorro, M., Williams, I. S., Silva, J. B., Fernández, C., Diaz-Azpiroz, M., Apraiz, A. and Castro, A.: Variscan intra-orogenic extensional tectonics in the Ossa – Morena-Évora – Aracena – Lora del Río metamorphic belt , SW Iberian Zone (E Massif): SHRIMP zircon U – Th – Pb geochronology, in Ancient Orogens and Modern Analogues, edited by J. B. Murphy, J. D. Keppie, and A. J. Hynes, pp. 327, 215–237, Geological Society of Londos, Special Publications., 2009.

Pereira, M. F., Ribeiro, C., Vilallonga, F., Chichorro, M., Drost, K., Silva, J. B., Albardeiro, L., Hofmann, M. and Linnemann, U.: Variability over time in the sources of South Portuguese Zone turbidites: Evidence of denudation of different crustal blocks during the assembly of Pangaea, Int. J. Earth Sci., 103(5), 1453–1470, doi:10.1007/s00531-013-0902-8, 2014.

Pérez-Cáceres, I., Martínez Poyatos, D., Simancas, J. F. and Azor, A.: The elusive nature of the Rheic Ocean suture in SW Iberia, Tectonics, 34(12), 2429–2450, doi:10.1002/2015TC003947, 2015.

Pérez-Cáceres, I., Simancas, J. F., Martínez Poyatos, D., Azor, A. and González Lodeiro, F.: Oblique collision and deformation partitioning in the SW Iberian Variscides, Solid Earth, 7(3), 857–872, doi:10.5194/se-7-857-2016, 2016.

Pérez-Estaún, A., Bastida, F., Alonso, J. L., Marquínez, J., Aller, J., Alvarez-Marrón, J., Marcos, A. and Pulgar, J. A.: A thin-skinned tectonics model for an arcuate fold and thrust belt: The Cantabrian Zone (Variscan Ibero-Armorican Arc), Tectonics, 7(3), 517–537, doi:https://doi.org/10.1029/TC007i003p00517, 1988.

Pérez-Estaún, A., Bastida, F., Martínez Catalán, J.R. Gutierrez Marco, J. C., Marcos, A. and Pulgar, J. .: West Asturian-Leonese Zone. Stratigraphy, in Pre-Mesozoic Geology of Iberia, edited by E. Dallmeyer, R.D. and Martínez Garcia, pp. 92–102, Springer-Verlag, Berlin., 1990.

Pérez-Estaún, A., Martínez Catalán, J. R. and Bastida, F.: Crustal thickening and deformation

1383 sequence in the footwall to the suture of the Variscan belt of northwest Spain, Tectonophysics,
1384 191(3–4), 243–253, doi:10.1016/0040-1951(91)90060-6, 1991.

1385 Pérez-Estaún, A., Pulgar, J. A., Banda, E. and Alvarez-Marrón, J.: Crustal structure of the
1386 external variscides in northwest spain from deep seismic reflection profiling, Tectonophysics,
1387 232(1–4), doi:10.1016/0040-1951(94)90078-7, 1994.

1388 Pin, C., Fonseca, P. E., Paquette, J. L., Castro, P. and Matte, P.: The ca. 350 Ma Beja Igneous
1389 Complex: A record of transcurrent slab break-off in the Southern Iberia Variscan Belt?,
1390 Tectonophysics, 461(1–4), 356–377, doi:10.1016/j.tecto.2008.06.001, 2008.

1391 Pulgar, J. A., Gallart, J., Fernández-Viejo, G., Pérez-Estaún, A. and Álvarez-Marrón, J.: Seismic
1392 image of the Cantabrian Mountains in the western extension of the Pyrenees from integrated
1393 ESCIN reflection and refraction data, Tectonophysics, 264(1–4), 1–19, doi:10.1016/S0040-
1394 1951(96)00114-X, 1996.

1395 Quesada, C. and Dallmeyer, R. D.: Tectonothermal evolution of the Badajoz-Cordóba shear
1396 zone (SW Iberia): characteristics and 40Ar/39Ar mineral age constraints, Tectonophysics,
1397 231(1–3), 195–213, doi:10.1016/0040-1951(94)90130-9, 1994.

1398 Quintana, L., Pulgar, J. A. and Alonso, J. L.: Displacement transfer from borders to interior of a
1399 plate: A crustal transect of Iberia, Tectonophysics, 663, 378–398,
1400 doi:10.1016/j.tecto.2015.08.046, 2015.

1401 Rat, P.: The Basque-Cantabrian basin between the Iberian and European plates: Some facts but
1402 still many problems, Rev. la Soc. Geológica España, 1(3–4), 327–348, 1988.

1403 Reche, J., Martinez, F. J., Arboleya, M. L., Dietsch, C. and Briggs, W. D.: Evolution of a kyanite-
1404 bearing belt within a HT-LP orogen: the case of NW Variscan Iberia, J. Metamorph. Geol., 16(3),
1405 379–394, doi:10.1111/j.1525-1314.1998.00142.x, 1998.

1406 Ries, A. C. and Shackleton, R. M.: Catazonal Complexes of North-West Spain and North
1407 Portugal, Remnants of a Hercynian Thrust Plate, Nat. Phys. Sci., 234(47), 65–68,
1408 doi:10.1038/physci234065a0, 1971.

1409 Robardet, M.: Alternative approach to the Variscan Belt in southwestern Europe: Preorogenic
1410 paleobiogeographical constraints, Spec. Pap. Geol. Soc. Am., 364, 1–15, doi:10.1130/0-8137-
1411 2364-7.1, 2002.

1412 Robardet, M. and Gutiérrez Marco, J. C.: Ossa-Morena Zone. Stratigraphy. Passive Margin
1413 Phase (Ordovician-Silurian-Devonian), in Pre-Mesozoic Geology of Iberia, edited by R. D.
1414 Dallmeyer and E. Martínez García, pp. 267–272, Springer-Verlag, Berlin., 1990.

1415 Rodrigues, B., Chew, D. M., Jorge, R. C. G. S., Fernandes, P., Veiga-Pires, C. and Oliveira, J. T.:
1416 Detrital zircon geochronology of the Carboniferous Baixo Alentejo Flysch Group (South
1417 Portugal); Constraints on the provenance and geodynamic evolution of the South Portuguese
1418 Zone, J. Geol. Soc. London., 172, 294–308, doi:10.1144/jgs2013-084, 2015.

1419 Ross, A. R., Brown, L. D., Pananont, P., Nelson, K. D., Klemperer, S. L., Haines, S., Wenjin, Z. and
1420 Jingru, G.: Deep reflection surveying in central Tibet: Lower-crustal layering and crustal flow,
1421 Geophys. J. Int., 156(1), 115–128, doi:10.1111/j.1365-246X.2004.02119.x, 2004.

1422 Royden, L.: Coupling and decoupling of crust and mantle in convergent orogens: Implications
1423 for strain partitioning in the crust, J. Geophys. Res., 101(B8), 17679–17705, 1996.

1424 Rubio Pascual, F. J., Arenas, R., Martínez Catalán, J. R., Rodríguez Fernández, L. R. and
1425 Wijbrans, J. R.: Thickening and exhumation of the Variscan roots in the Iberian Central System:
1426 Tectonothermal processes and 40Ar/39Ar ages, Tectonophysics, 587, 207–221,
1427 doi:10.1016/j.tecto.2012.10.005, 2013.

1428 Sánchez-García, T., Quesada, C., Bellido, F., Dunning, G. R. and González del Tánago, J.: Two-
1429 step magma flooding of the upper crust during rifting: The Early Paleozoic of the Ossa Morena
1430 Zone (SW Iberia), Tectonophysics, 461(1–4), 72–90, doi:10.1016/j.tecto.2008.03.006, 2008.

1431 Sánchez-García, T., Bellido, F., Pereira, M. F., Chichorro, M., Quesada, C., Pin, C. and Silva, J. B.:
1432 Rift-related volcanism predating the birth of the Rheic Ocean (Ossa-Morena zone, SW Iberia),
1433 Gondwana Res., 17(2–3), 392–407, doi:10.1016/j.gr.2009.10.005, 2010.

1434 Sánchez de Posada, L. C., Martínez Chacón, M. L., Méndez Fernández, C., Menéndez Alvarez,
1435 J.R. Truyols, J. and Villa, E.: Carboniferous Pre-Stephanian rocks of the Asturian-Leonese
1436 Domain (Cantabrian Zone), in Pre-Mesozoic Geology of Iberia, edited by R. D. Dallmeyer and E.
1437 Martínez García, pp. 24–33, Springer-Verlag., 1990.

1438 Sánchez Martínez, S., Arenas, R., Andonaegui, P., Martínez Catalán, J. R. and Pearce, J. A.:
1439 Geochemistry of two associated ophiolites from the Cabo Ortegal Complex (Variscan belt of
1440 NW Spain), Mem. Geol. Soc. Am., 200(23), 445–467, doi:10.1130/2007.1200(23), 2007.

1441 Schmelzbach, C., Juhlin, C., Carbonell, R. and Simancas, J. F.: Prestack and poststack migration
1442 of crooked-line seismic reflection data: A case study from the South Portuguese Zone fold belt,
1443 southwestern Iberia, Geophysics, 72(2), 9–18, doi:10.1190/1.2407267, 2007.

1444 Schmelzbach, C., Simancas, J. F., Juhlin, C. and Carbonell, R.: Seismic reflection imaging over
1445 the South Portuguese Zone fold-and-thrust belt, SW Iberia, J. Geophys. Res. Solid Earth, 113(8),
1446 1–16, doi:10.1029/2007JB005341, 2008.

1447 Seyferth, M. and Henk, A.: Syn-convergent exhumation and lateral extrusion in continental
1448 collision zones - Insights from three-dimensional numerical models, Tectonophysics, 382(1–2),
1449 1–29, doi:10.1016/j.tecto.2003.12.004, 2004.

1450 Shelley, D. and Bossière, G.: A new model for the Hercynian Orogen of Gondwanan France and
1451 Iberia, J. Struct. Geol., 22(6), 757–776, doi:10.1016/S0191-8141(00)00007-9, 2000.

1452 Simancas, J. F., Martínez Poyatos, D., Expósito, I., Azor, A. and González Lodeiro, F.: The
1453 structure of a major suture zone in the SW iberian massif: The Ossa-Morena/central iberian
1454 contact, Tectonophysics, 332(1–2), 295–308, doi:10.1016/S0040-1951(00)00262-6, 2001.

1455 Simancas, J. F., Carbonell, R., González Lodeiro, F., Pérez-Estaún, A., Juhlin, C., Ayarza, P.,
1456 Kashubin, A., Azor, A., Martínez Poyatos, D., Almodóvar, G. R., Pascual, E., Sáez, R. and
1457 Expósito, I.: Crustal structure of the transpressional Variscan orogen of SW Iberia: SW Iberia
1458 deep seismic reflection profile (IBERSEIS), Tectonics, 22(6), doi:10.1029/2002TC001479, 2003.

1459 Simancas, J. F., Carbonell, R., Gonzalez Lodeiro, F., Pérez-Estaún, A., Juhlin, C., Ayarza, P.,
1460 Kashubin, A., Azor, A., Martínez Poyatos, D., Saez, R., Almodovar, G. R., Pascual, E., Flecha, I.
1461 and Marti, D.: Transpressional collision tectonics and mantle plume dynamics: the Variscides of
1462 southwestern Iberia, Geol. Soc. London, Mem., 32(1), 345–354, 2006.

1463 Simancas, J. F., Ayarza, P., Azor, A., Carbonell, R., Martínez Poyatos, D., Pérez-Estaún, A. and
1464 González Lodeiro, F.: A seismic geotraverse across the Iberian Variscides: Orogenic shortening,
1465 collisional magmatism, and orocline development, Tectonics, 32(3), 417–432,
1466 doi:10.1002/tect.20035, 2013.

Snelson, C. M., Randy Keller, G., Miller, K. C., Rumpel, H. M. and Prodehl, C.: Regional Crustal Structure Derived from the CD-ROM 99 Seismic Refraction/Wide-Angle Reflection Profile: The Lower Crust and Upper Mantle, in The Rocky Mountain Region: An Evolving Lithosphere: Tectonics, Geochemistry, and Geophysics, pp. 271–291., 2013.

Spear, F. S.: Metamorphic Phase Equilibria and pressure-temperature-time paths, Monograph., edited by M. Mineralogical Society of America, Chelsea., 1993.

Stille, H.: Grundfragen der Vergleichenden. Tectonik, Gebrueder Borntragen, Berlin., 1924.

Taner, M. T. and Sheriff, R. E.: Application of Amplitude, Frequency, and Other Attributes to Stratigraphic and Hydrocarbon Determination, in AAPG Memoir, Seismic Stratigraphy — Applications to Hydrocarbon Exploration, vol. 26, pp. 301–327., 1977.

Teixell, A., Labaume, P., Ayarza, P., Espurt, N., de Saint Blanquat, M. and Lagabrielle, Y.: Crustal structure and evolution of the Pyrenean-Cantabrian belt: A review and new interpretations from recent concepts and data, Tectonophysics, 724–725(July 2017), 146–170, doi:10.1016/j.tecto.2018.01.009, 2018.

Truyols, J., Arbizu, M., Garcia-Alcalde, J. L., Garcia-López, S., Mendez-Bendia, I., Soto, F. and Truyols, M.: The Asturian-Leonese Domain (Cantabrian Zone), in Pre-Mesozoic Geology of Iberia, edited by R. D. Dallmeyer and E. Martínez García, pp. 10–19, Springer-Verlag., 1990.

de Vicente, G., Giner, J. L., Muñoz-Martí, A., González-Casado, J. M. and Lindo, R.: Determination of present-day stress tensor and neotectonic interval in the Spanish Central System and Madrid Basin, central Spain, Tectonophysics, 266(1–4), 405–424, doi:10.1016/S0040-1951(96)00200-4, 1996.

Villaseca, C., Orejana, D. and Belousova, E. A.: Recycled metaigneous crustal sources for S- and I-type Variscan granitoids from the Spanish Central System batholith: Constraints from Hf isotope zircon composition, Lithos, 153, 84–93, doi:10.1016/j.lithos.2012.03.024, 2012.

Wever, T.: The Conrad discontinuity and the top of the reflective lower crust-do they coincide?, Tectonophysics, 157(1–3), 39–58, doi:10.1016/0040-1951(89)90339-9, 1989.

Xiaobo, H. and Tae Kyung, H.: Evidence for strong ground motion by waves refracted from the Conrad discontinuity, Bull. Seismol. Soc. Am., 100(3), 1370–1374, doi:10.1785/0120090159, 2010.

Table 1: Acquisition parameters of the NI seismic profiles shown from figures 3 to 8 and former processing flows. These are grouped according to their similarities.

Acquisition parameters	**ESCIN-1 (onshore)**	**ESCIN-2 (onshore)**
Source	Dynamite-single-hole	Dynamite-single-hole
Charge	20 kg at 24 m depth	20 kg at 24 m depth
Trace Interval	60 m	60 m
# of traces	240	240
Spread configuration	Symmetrical Split-spread	Symmetrical Split-spread
Fold	30	30
Geophones per group	18	18

Spread length	14.5 km	14.5 km
Sample rate	4 ms	4 ms
Kirchoff time migration	5600 m/s	5600 m/s

	ESCIN-3.2 and ESCIN-3.3 (offshore)
Source	Airgun (5490 cu.in)
Shot spacing	75 m
Receiver interval	12.5 m
Spread length	4500 m
Fold	30
Internal offset	240 m
Sample rate	4 ms
Record length	20 s
Kirchoff time migration	5200 m/s

	IBERSEIS (onshore)	**ALCUDIA (onshore)**
Source	4, 22T vibrators	4 (+1), 22T vibrators
Recording instrument	SERCEL 388, 10 Hz	SERCEL 388, 10 Hz
# active channels	240 minimum	240 minimum
Station spacing	35 m	35 m
Station configuration	12 geophones	12 geophones
Source spacing	70 m	70 m
Sweep frequencies	non-linear 8-80 Hz	non-linear 8-80 Hz
Sweep length	20 s	20 s
Listening time	40 s	40 s
Sample rate	2 ms	4 ms
Spread type	Asymmetric split-spread	Asymmetric split-spread
Nominal fold	60 (minimum)	60 (minimum)
Kirchoff time migration	6000 m/s	6200 m/s

Figure captions

Figure 1: (a) Map of the Iberian Peninsula showing the outcrops of the Variscan basement and the subdivision in zones of the Iberian Massif. The main strike-slip shear zones, traces of Variscan folds and gneiss domes are also included. Blue lines show the position of normal incidence seismic reflection profiles and that of the CIMDEF transect. See legend for abbreviations. (b) Map of the outcropping granitoids in the Iberian Peninsula together with the main structures.

Figure 2: Processing flow carried over the SEG-Y original stack sections. This task was geared to improve and homogenize the resolution of the seismic images while creating new migrated sections. See Martínez García, (2019) for further details.

Figure 3: Cross-section (a) and depth converted time migrated section (v=5600 m/s) along the NI seismic profile ESCIN-1 (Fig. 1), without (b) and with interpretation (c). A sketch of the most important features is presented in (d). CDP: Common Depth Point. TWT: Two-way travel time. WALZ: West Asturian-Leonese Zone. CZ: Cantabrian Zone. The position of the

Narcea Antiform is indicated. Red dashed lines represent the boundaries provided by chaos and variance attribute analyses. Nomenclature for reflections goes as follows: (ot), outcropping thrusts; (t), thrusts affecting the basement; (b), indifferentiated basement; (st), sole thrust; (c), top of the lower crust; (ir), lower crust internal reflectivity; (m) is the Moho; (mig) are curved features resulting from the migration of discontinuous reflections. Depth conversion is based on migration velocities.

Figure 4: Cross-section ((a) modified from Gallastegui et al., 2016) and depth converted time migrated section (v=5600 m/s) of the NI seismic profile ESCIN-2 (Fig. 1), without (b) and with interpretation (c). A sketch of the most important features is presented in (d). A 1D velocity profile as modeled from wide-angle data (Pulgar et al., 1996) appears in (e). CDP: Common Depth Point. TWT: Two-way travel time. CZ: Cantabrian Zone. Some discontinuous reflections are traced on the basis of their geometry on the stack image (Pulgar et al., 1996). Red dashed lines represent the boundaries provided by chaos and variance attribute analyses. (s), sediments; (t), thrusts; (ot), outcropping thrusts; (ps), Paleozoic sediments; (c), top of the lower crust; (lc), lower crust; (m), Moho. Depth conversion is based on migration velocities.

Figure 5: Cross-section (a) and depth converted time migrated section (v=5200 m/s) of the NI seismic profile ESCIN-3.3 (Fig. 1), without (b) and with interpretation (c). A sketch of the most important features is presented in (d). A 1D velocity profile as modeled from wide-angle data (Ayarza et al., 1998) in presented in (e). CDP: Common Depth Point. TWT: Two-way travel time. CZ: Cantabrian Zone. WALZ: West Asturian-Leonese Zone. CIZ: Central Iberian Zone. The offshore projection of the Viveiro Fault is indicated. Red dashed lines represent the boundaries provided by chaos and variance attribute analyses. (s), sediments; (t), thrusts; (st), sole thrust; (ef), extensional features; (c), top of the lower crust; (lc), lower crust; (ir) lower crust internal reflectivity; (m), Moho; (sc), subcrustal reflections; (mig) curved features resulting from the migration of discontinuous reflections. Depth conversion is based on migration velocities.

Figure 6: Cross-section (a) and depth converted time migrated section (v=5200 m/s) of the NI seismic profile ESCIN-3.2 (Fig. 1), without (b) and with interpretation (c). A sketch of the most important features is presented in (d). CDP: Common Depth Point. TWT: Two-way travel time. GTMZ: Galicia-Trás-os-Montes Zone. CIZ: Central Iberian Zone. (s), sediments; (ef), extensional features; (lc), lower crust; (m), Moho; (sc), subcrustal reflections; (czlc) CZ underthrusted lower crust. Depth conversion is based on migration velocities.

Figure 7: Cross-section ((a) modified from Martínez Poyatos et al., 2012) and depth converted time migrated section (v=6200 m/s) of the NI seismic profile ALCUDIA (Fig. 1), without (b) and with interpretation (c). A sketch of the most important features is presented in (d). A 1D velocity profile as modeled from wide-angle data (Palomeras et al., in press) is overlapped in (d). CDP: Common Depth Point. TWT: Two-way travel time. CIZ: Central Iberian Zone. OMZ: Ossa-Morena Zone. (cu): Central Unit; (vf): vertical folds; (g): granites; (ef): extensional features; (c): top of the lower crust; (lc): lower crust; (cc) and (cc'): crocodile structure; (m): Moho. Red dashed lines represent the boundaries provided by chaos and variance attribute analyses. Depth conversion is based on migration velocities.

Figure 8: Cross-section ((a), modified from Simancas et al., 2003) and depth converted time migrated section (v=6000 m/s) of the NI seismic profile IBERSEIS (Fig. 1), without (b) and with interpretation (c). A sketch of the most important features is presented in (d). Two 1D velocity profiles as modeled from wide-angle data (Palomeras et al., 2009)are overlapped in (d). CDP: Common Depth Point. TWT: Two-way travel time. CIZ: Central Iberian Zone. OMZ: Ossa-Morena Zone. SPZ: South Portuguese Zone. (t), thrusts; (ot), outcropping thrusts; (irb), Iberseis Reflective Body; (c), top of the lower crust; (lc), lower crust; (ir) lower crust internal reflectivity; (lct), lower crust thrusts; (m), Moho. Depth conversion is based on migration velocities.

Figure 9: Joint geological interpretation of all the seismic sections (normal incidence and seismic noise) whose location is shown in figure 1. (a): ESCIN-1, ESCIN3-3 and ESCIN-3.2. (b): ALCUDIA and IBERSEIS. (c): CIMDEF (Andrés et al., 2020). Special attention should be paid to the depth and geometry of the Moho and mid-crustal discontinuity. Alpine structures (i.e. crustal thickening) appear in ESCIN-1 and in CIMDEF. The rest are Variscan features.

Figure 10: Map of the Moho depth as derived from tomography of shear waves (seismic noise and earthquakes, Palomeras et al., 2017) with the projection of the seismic profiles already shown in figure 1 and described along the text. A sketch of the geometry of the main discontinuities (Moho and Conrad) is also shown.

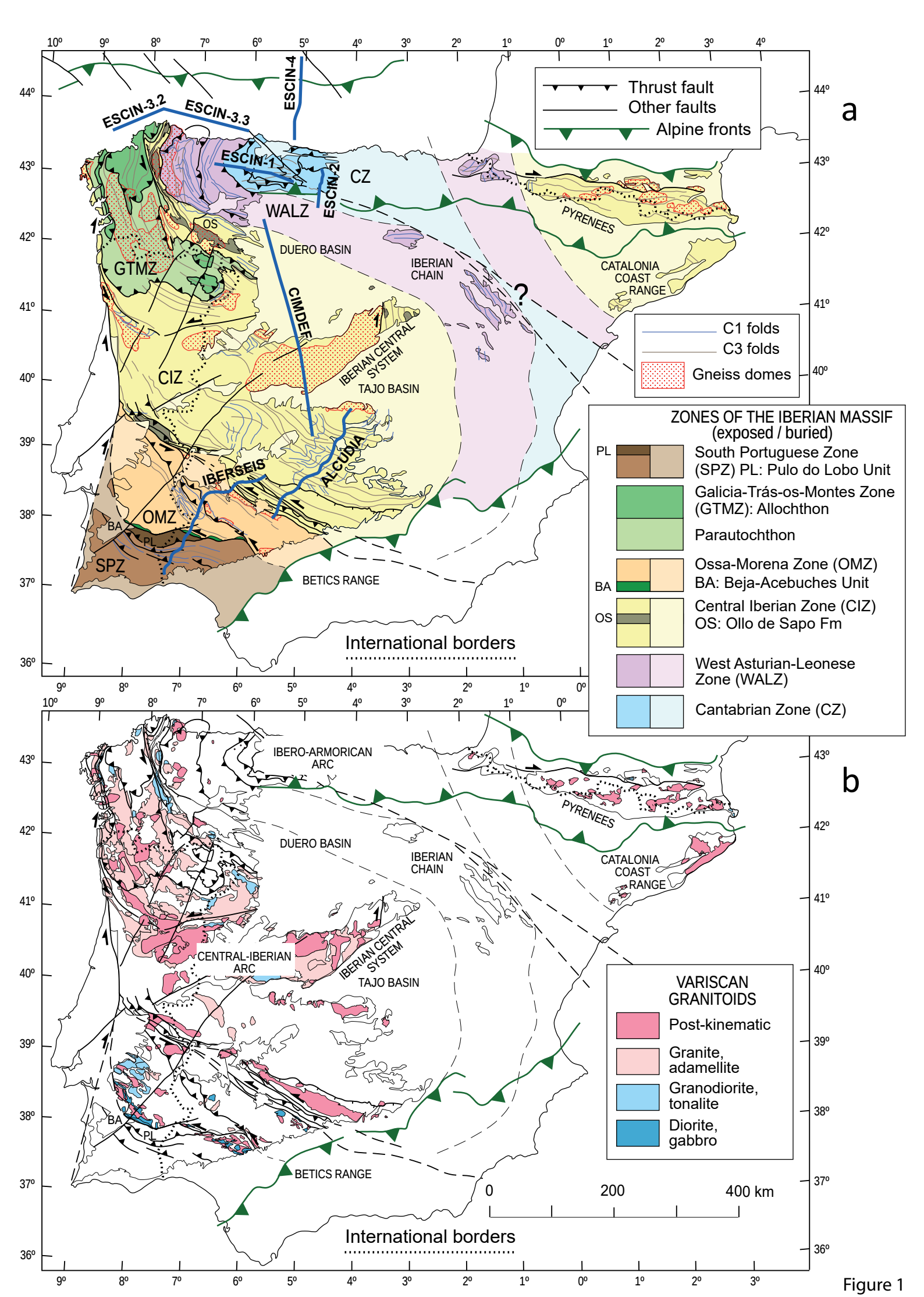
a
Thrust fault
Other faults
Alpine fronts
ESCIN-4
ESCIN-3.2
ESCIN-3.3
ESCIN-1
ESCIN-2
CZ
WALZ
OS
DUERO BASIN
GTMZ
CIMDE
IBERIAN CHAIN
PYRENEES
CATALONIA COAST RANGE
?
C1 folds
C3 folds
Gneiss domes
IBERIAN CENTRAL SYSTEM
TAJO BASIN
CIZ
ALCUDIA
IBERSEIS
OMZ
BA
PL
SPZ
BETICS RANGE
International borders
ZONES OF THE IBERIAN MASSIF
(exposed / buried)
PL
South Portuguese Zone (SPZ) PL: Pulo do Lobo Unit
Galicia-Trás-os-Montes Zone (GTMZ): Allochthon
Parautochthon
Ossa-Morena Zone (OMZ)
BA
BA: Beja-Acebuches Unit
OS
Central Iberian Zone (CIZ)
OS: Ollo de Sapo Fm
West Asturian-Leonese Zone (WALZ)
Cantabrian Zone (CZ)
b
IBERO-ARMORICAN ARC
DUERO BASIN
IBERIAN CHAIN
PYRENEES
CATALONIA COAST RANGE
CENTRAL-IBERIAN ARC
IBERIAN CENTRAL SYSTEM
TAJO BASIN
BA
PL
BETICS RANGE
VARISCAN GRANITOIDS
Post-kinematic
Granite, adamellite
Granodiorite, tonalite
Diorite, gabbro
0
200
400 km
International borders

Figure 1

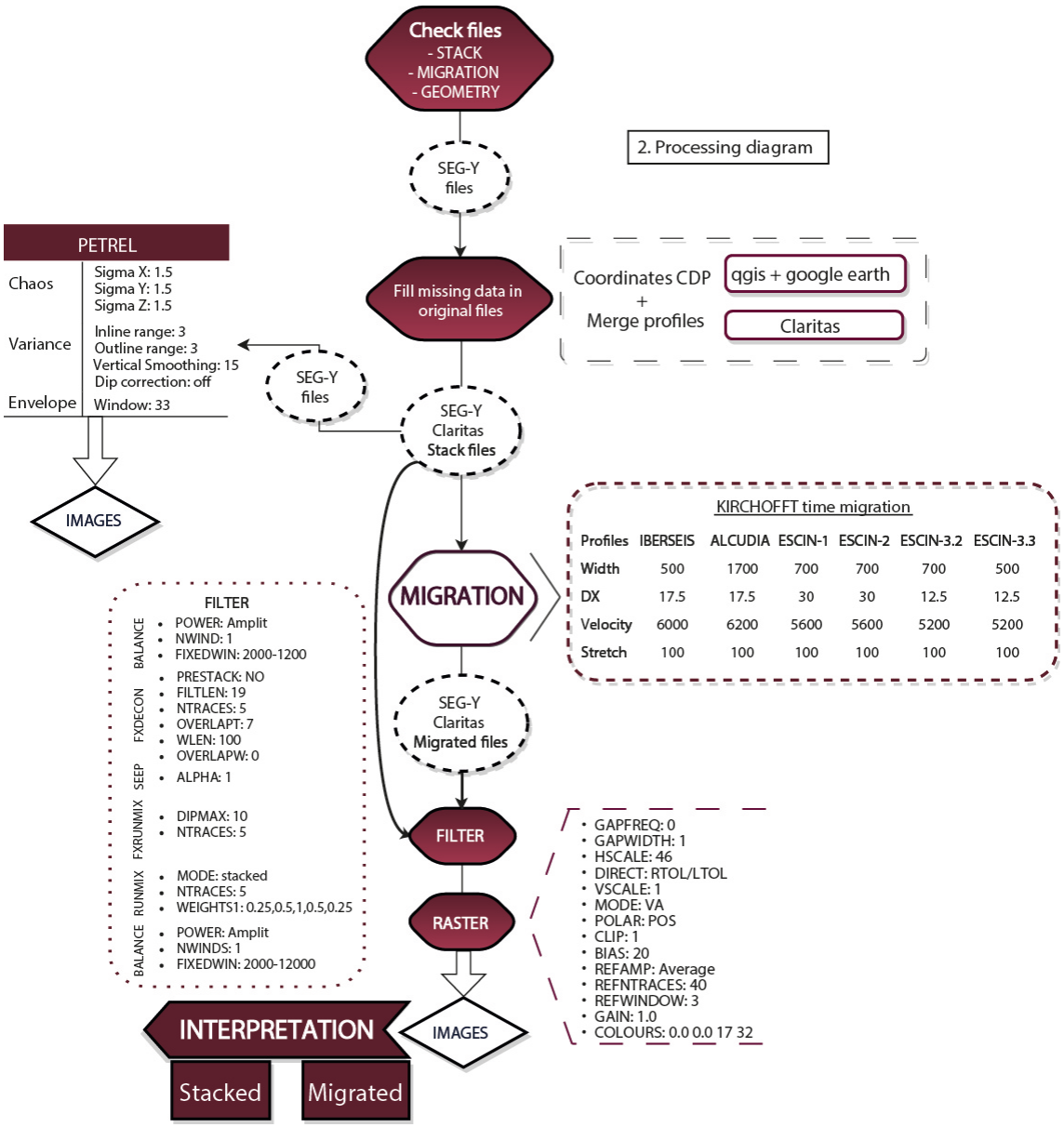
Check files
- STACK
- MIGRATION
- GEOMETRY
SEG-Y files
2. Processing diagram
Fill missing data in original files
Coordinates CDP
+
Merge profiles
qgis + google earth
Claritas
PETREL
Chaos
Sigma X: 1.5
Sigma Y: 1.5
Sigma Z: 1.5
Variance
Inline range: 3
Outline range: 3
Vertical Smoothing: 15
Dip correction: off
Envelope
Window: 33
SEG-Y files
SEG-Y Claritas Stack files
IMAGES
KIRCHOFFT time migration
Profiles IBERSEIS ALCUDIA ESCIN-1 ESCIN-2 ESCIN-3.2 ESCIN-3.3
Width 500 1700 700 700 700 500
DX 17.5 17.5 30 30 12.5 12.5
Velocity 6000 6200 5600 5600 5200 5200
Stretch 100 100 100 100 100 100
MIGRATION
FILTER
BALANCE
POWER: Amplit
NWIND: 1
FIXEDWIN: 2000-1200
FXDECON
PRESTACK: NO
FILTLEN: 19
NTRACES: 5
OVERLAPT: 7
WLEN: 100
OVERLAPW: 0
SEEP
ALPHA: 1
FXRUNMIX
DIPMAX: 10
NTRACES: 5
RUNMIX
MODE: stacked
NTRACES: 5
WEIGHTS1: 0.25,0.5,1,0.5,0.25
BALANCE
POWER: Amplit
NWINDS: 1
FIXEDWIN: 2000-12000
SEG-Y Claritas Migrated files
FILTER
RASTER
GAPFREQ: 0
GAPWIDTH: 1
HSCALE: 46
DIRECT: RTOL/LTOL
VSCALE: 1
MODE: VA
POLAR: POS
CLIP: 1
BIAS: 20
REFAMP: Average
REFNTRACES: 40
REFWINDOW: 3
GAIN: 1.0
COLOURS: 0.0 0.0 17 32
IMAGES
INTERPRETATION
Stacked
Migrated

Figure 2

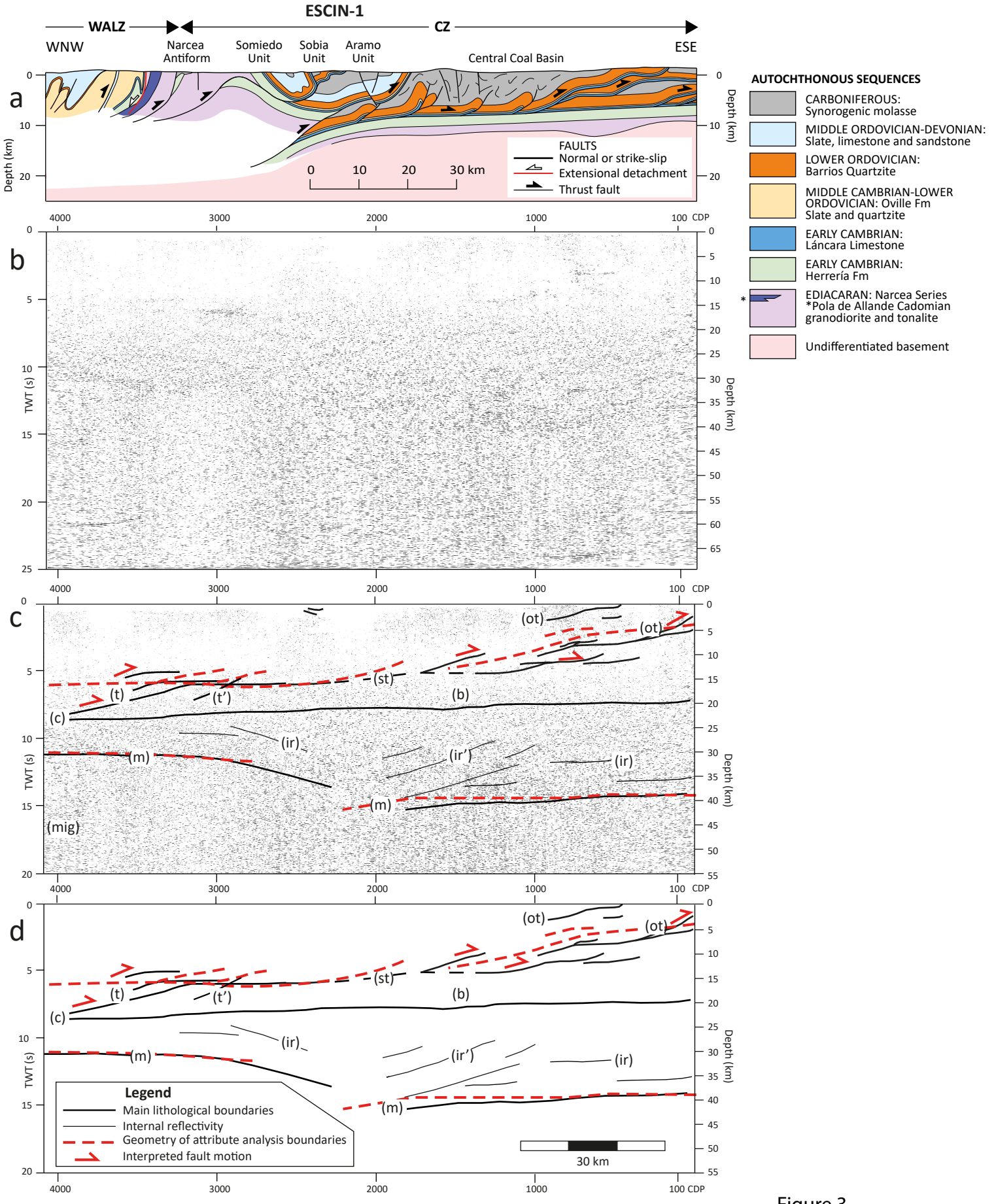
ESCIN-1
WALZ
CZ
WNW
ESE
Narcea Antiform
Somiedo Unit
Sobia Unit
Aramo Unit
Central Coal Basin
a
Depth (km)
FAULTS
Normal or strike-slip
Extensional detachment
Thrust fault
0 10 20 30 km
AUTOCHTHONOUS SEQUENCES
CARBONIFEROUS: Synorogenic molasse
MIDDLE ORDOVICIAN-DEVONIAN: Slate, limestone and sandstone
LOWER ORDOVICIAN: Barrios Quartzite
MIDDLE CAMBRIAN-LOWER ORDOVICIAN: Oville Fm Slate and quartzite
EARLY CAMBRIAN: Láncara Limestone
EARLY CAMBRIAN: Herrería Fm
EDIACARAN: Narcea Series
*Pola de Allande Cadomian granodiorite and tonalite
Undifferentiated basement
4000 3000 2000 1000 100 CDP
b
TWT (s)
Depth (km)
c
(ot)
(st)
(t)
(t')
(b)
(c)
(ir)
(ir')
(m)
(mig)
d
Legend
Main lithological boundaries
Internal reflectivity
Geometry of attribute analysis boundaries
Interpreted fault motion
30 km

Figure 3

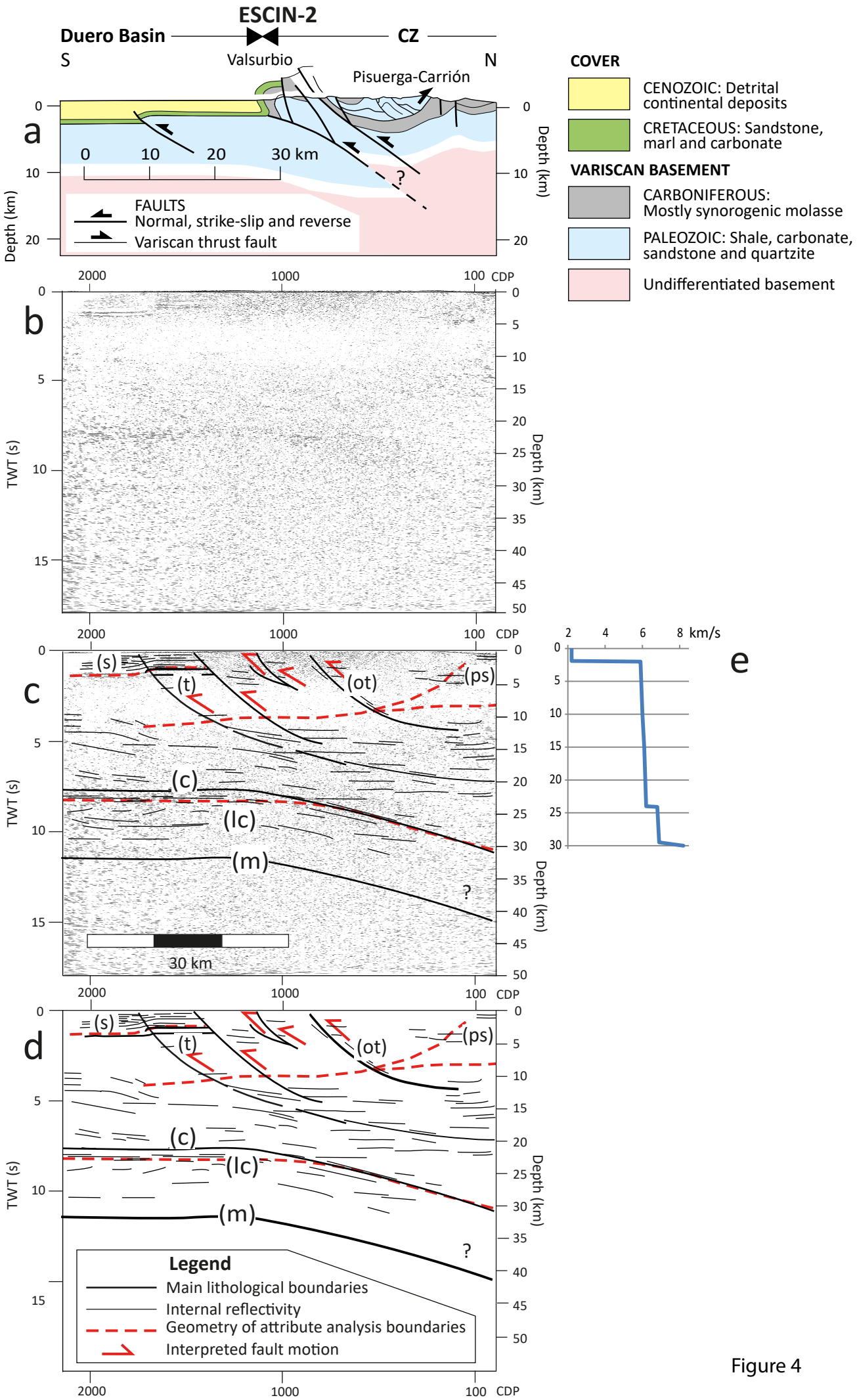
ESCIN-2
Duero Basin
CZ
S
N
Valsurbio
Pisuerga-Carrión
a
0
10
20
30 km
?
Depth (km)
FAULTS
Normal, strike-slip and reverse
Variscan thrust fault
COVER
CENOZOIC: Detrital continental deposits
CRETACEOUS: Sandstone, marl and carbonate
VARISCAN BASEMENT
CARBONIFEROUS: Mostly synorogenic molasse
PALEOZOIC: Shale, carbonate, sandstone and quartzite
Undifferentiated basement
2000
1000
100 CDP
b
TWT (s)
Depth (km)
c
(s)
(t)
(ot)
(ps)
(c)
(lc)
(m)
?
30 km
d
e
2
4
6
8 km/s
Legend
Main lithological boundaries
Internal reflectivity
Geometry of attribute analysis boundaries
Interpreted fault motion

Figure 4

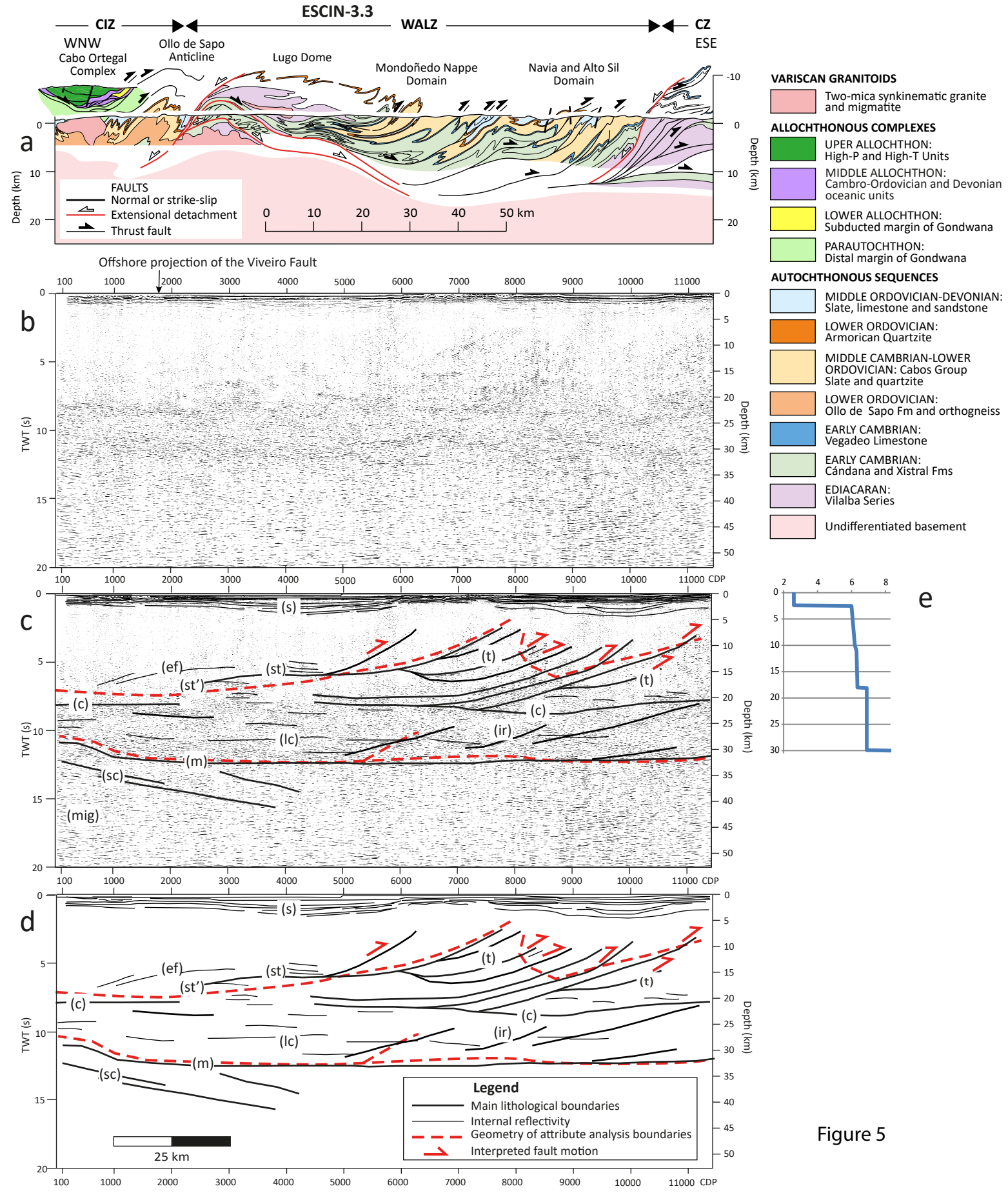
ESCIN-3.3
CIZ
WALZ
CZ
WNW
ESE
Cabo Ortegal Complex
Ollo de Sapo Anticline
Lugo Dome
Mondoñedo Nappe Domain
Navia and Alto Sil Domain
a
Depth (km)
FAULTS
Normal or strike-slip
Extensional detachment
Thrust fault
0 10 20 30 40 50 km
Offshore projection of the Viveiro Fault
b
TWT (s)
Depth (km)
CDP
c
(s)
(ef)
(st)
(st')
(t)
(c)
(lc)
(ir)
(m)
(sc)
(mig)
d
Legend
Main lithological boundaries
Internal reflectivity
Geometry of attribute analysis boundaries
Interpreted fault motion
25 km
VARISCAN GRANITOIDS
Two-mica synkinematic granite and migmatite
ALLOCHTHONOUS COMPLEXES
UPER ALLOCHTHON: High-P and High-T Units
MIDDLE ALLOCHTHON: Cambro-Ordovician and Devonian oceanic units
LOWER ALLOCHTHON: Subducted margin of Gondwana
PARAUTOCHTHON: Distal margin of Gondwana
AUTOCHTHONOUS SEQUENCES
MIDDLE ORDOVICIAN-DEVONIAN: Slate, limestone and sandstone
LOWER ORDOVICIAN: Armorican Quartzite
MIDDLE CAMBRIAN-LOWER ORDOVICIAN: Cabos Group Slate and quartzite
LOWER ORDOVICIAN: Ollo de Sapo Fm and orthogneiss
EARLY CAMBRIAN: Vegadeo Limestone
EARLY CAMBRIAN: Cándana and Xistral Fms
EDIACARAN: Vilalba Series
Undifferentiated basement
e

Figure 5

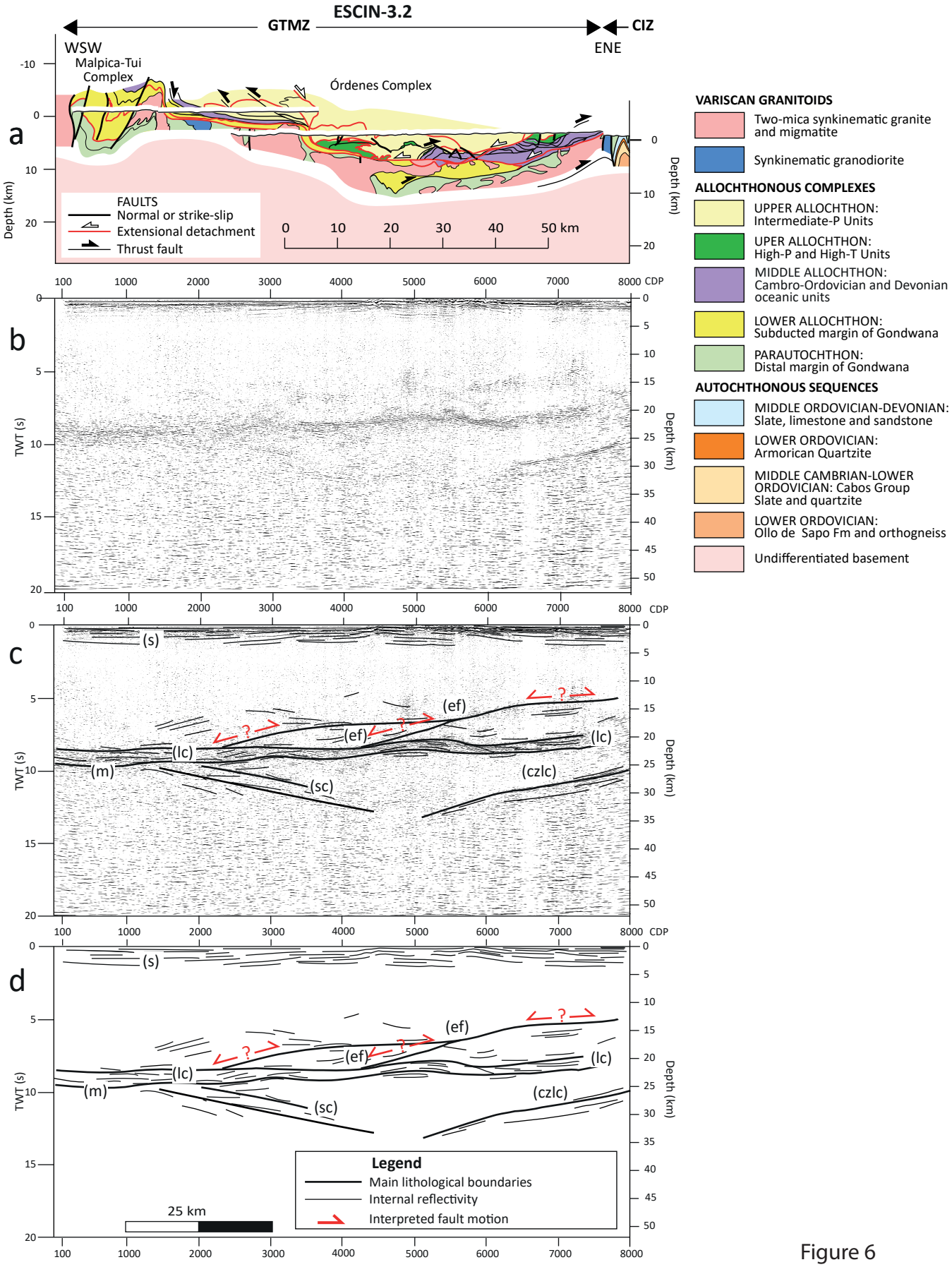
ESCIN-3.2
GTMZ
CIZ
WSW
ENE
Malpica-Tui Complex
Órdenes Complex
a
b
c
d
Depth (km)
TWT (s)
CDP
FAULTS
Normal or strike-slip
Extensional detachment
Thrust fault
0 10 20 30 40 50 km
(s)
(ef)
(lc)
(m)
(sc)
(czlc)
Legend
Main lithological boundaries
Internal reflectivity
Interpreted fault motion
25 km
VARISCAN GRANITOIDS
Two-mica synkinematic granite and migmatite
Synkinematic granodiorite
ALLOCHTHONOUS COMPLEXES
UPPER ALLOCHTHON: Intermediate-P Units
UPER ALLOCHTHON: High-P and High-T Units
MIDDLE ALLOCHTHON: Cambro-Ordovician and Devonian oceanic units
LOWER ALLOCHTHON: Subducted margin of Gondwana
PARAUTOCHTHON: Distal margin of Gondwana
AUTOCHTHONOUS SEQUENCES
MIDDLE ORDOVICIAN-DEVONIAN: Slate, limestone and sandstone
LOWER ORDOVICIAN: Armorican Quartzite
MIDDLE CAMBRIAN-LOWER ORDOVICIAN: Cabos Group Slate and quartzite
LOWER ORDOVICIAN: Ollo de Sapo Fm and orthogneiss
Undifferentiated basement

Figure 6

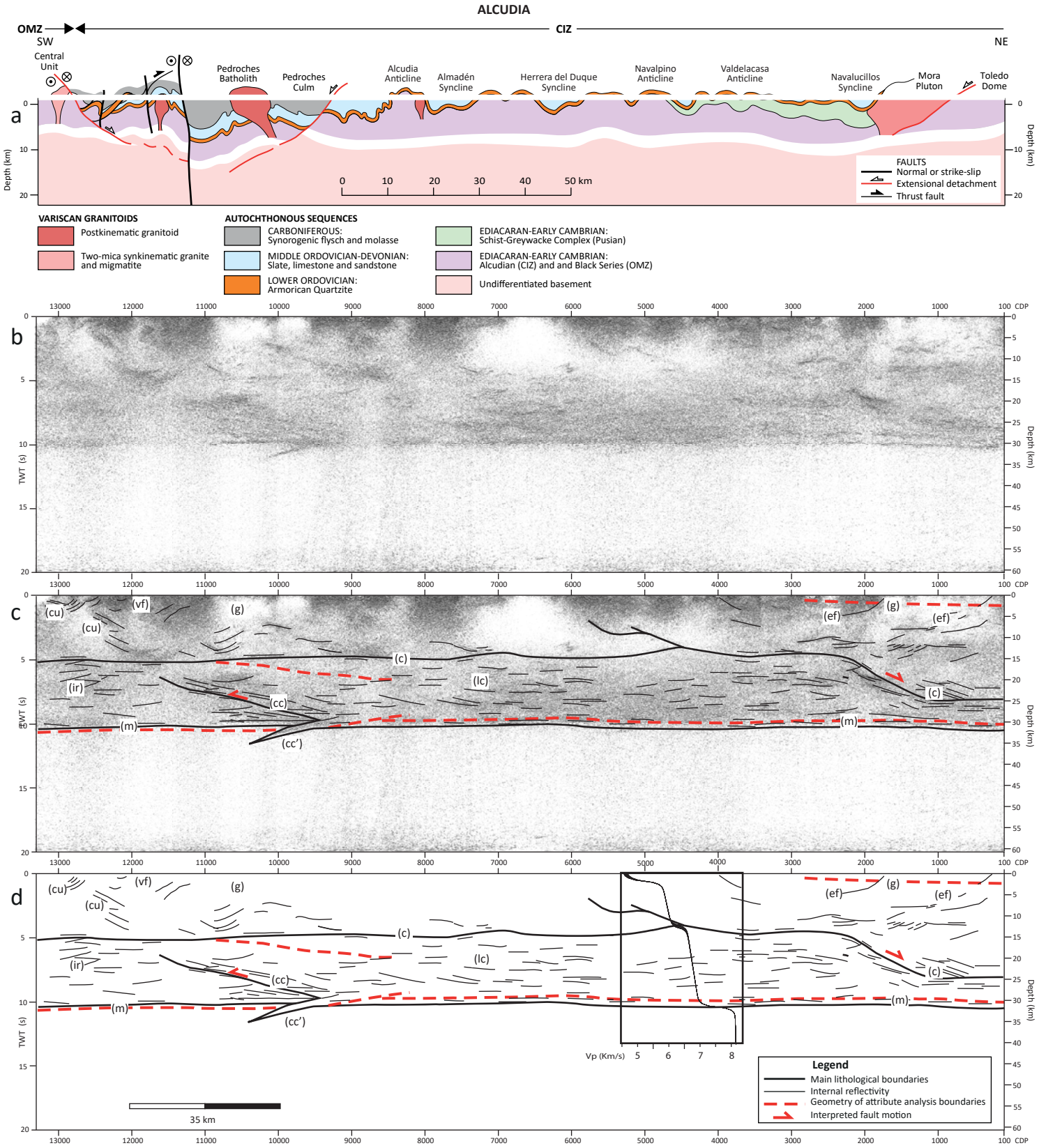
ALCUDIA
OMZ
CIZ
SW
NE
Central Unit
Pedroches Batholith
Pedroches Culm
Alcudia Anticline
Almadén Syncline
Herrera del Duque Syncline
Navalpino Anticline
Valdelacasa Anticline
Navalucillos Syncline
Mora Pluton
Toledo Dome
a
Depth (km)
0 10 20 30 40 50 km
FAULTS
Normal or strike-slip
Extensional detachment
Thrust fault
VARISCAN GRANITOIDS
Postkinematic granitoid
Two-mica synkinematic granite and migmatite
AUTOCHTHONOUS SEQUENCES
CARBONIFEROUS: Synorogenic flysch and molasse
MIDDLE ORDOVICIAN-DEVONIAN: Slate, limestone and sandstone
LOWER ORDOVICIAN: Armorican Quartzite
EDIACARAN-EARLY CAMBRIAN: Schist-Greywacke Complex (Pusian)
EDIACARAN-EARLY CAMBRIAN: Alcudian (CIZ) and and Black Series (OMZ)
Undifferentiated basement
b
c
d
TWT (s)
Depth (km)
CDP
(cu)
(vf)
(g)
(ef)
(c)
(ir)
(lc)
(cc)
(cc')
(m)
Vp (Km/s) 5 6 7 8
35 km
Legend
Main lithological boundaries
Internal reflectivity
Geometry of attribute analysis boundaries
Interpreted fault motion

Figure 7

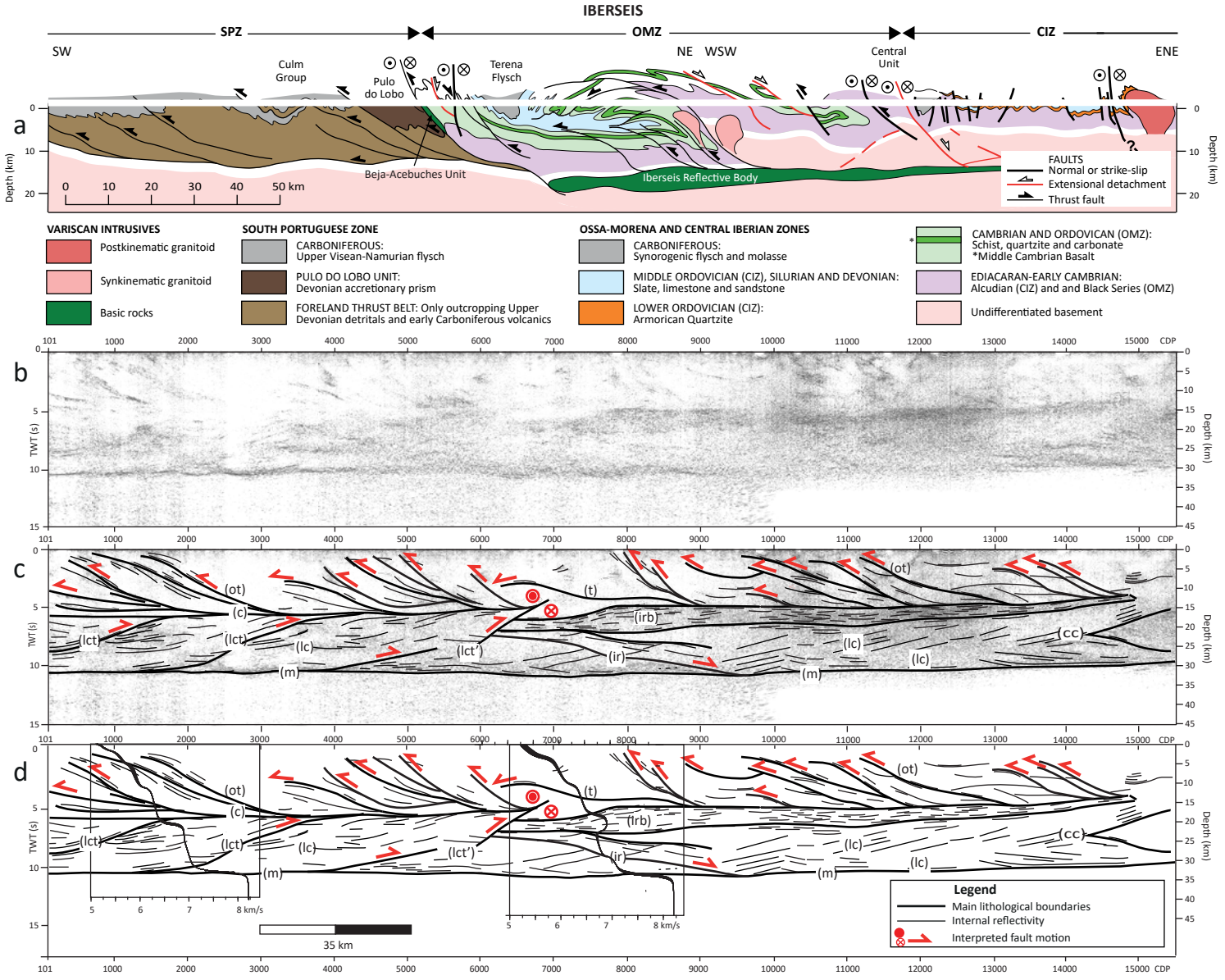
IBERSEIS
SPZ
OMZ
CIZ
SW
NE
WSW
ENE
Culm Group
Pulo do Lobo
Terena Flysch
Central Unit
a
Depth (km)
0 10 20 30 40 50 km
Beja-Acebuches Unit
Iberseis Reflective Body
FAULTS
Normal or strike-slip
Extensional detachment
Thrust fault
VARISCAN INTRUSIVES
Postkinematic granitoid
Synkinematic granitoid
Basic rocks
SOUTH PORTUGUESE ZONE
CARBONIFEROUS: Upper Visean-Namurian flysch
PULO DO LOBO UNIT: Devonian accretionary prism
FORELAND THRUST BELT: Only outcropping Upper Devonian detritals and early Carboniferous volcanics
OSSA-MORENA AND CENTRAL IBERIAN ZONES
CARBONIFEROUS: Synorogenic flysch and molasse
MIDDLE ORDOVICIAN (CIZ), SILURIAN AND DEVONIAN: Slate, limestone and sandstone
LOWER ORDOVICIAN (CIZ): Armorican Quartzite
CAMBRIAN AND ORDOVICAN (OMZ): Schist, quartzite and carbonate
*Middle Cambrian Basalt
EDIACARAN-EARLY CAMBRIAN: Alcudian (CIZ) and and Black Series (OMZ)
Undifferentiated basement
101 1000 2000 3000 4000 5000 6000 7000 8000 9000 10000 11000 12000 13000 14000 15000 CDP
b
TWT (s)
Depth (km)
c
(ot)
(c)
(lct)
(lc)
(m)
(t)
(irb)
(ir)
(lct')
(cc)
d
5 6 7 8 km/s
35 km
Legend
Main lithological boundaries
Internal reflectivity
Interpreted fault motion

Figure 8

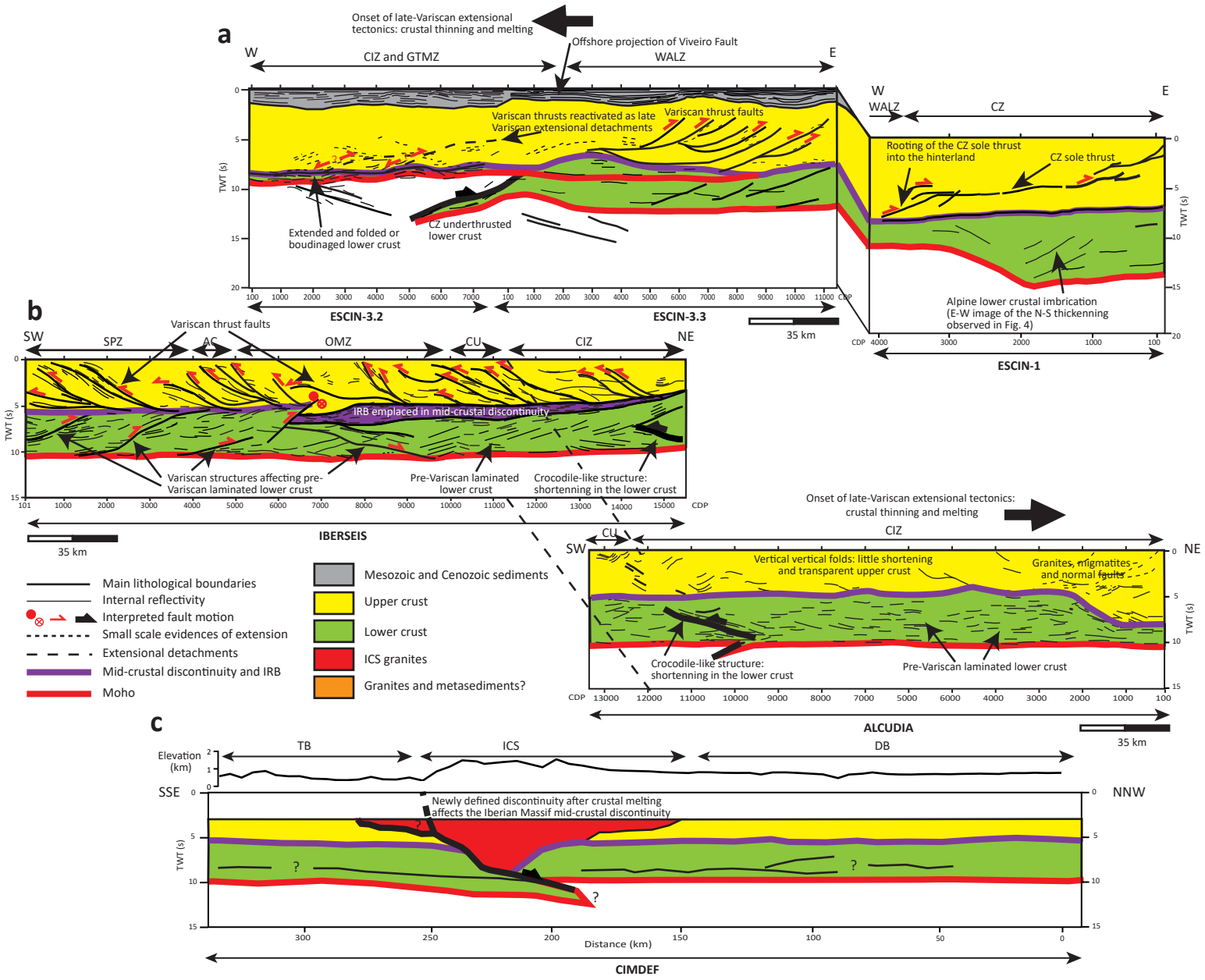
a
Onset of late-Variscan extensional tectonics: crustal thinning and melting
Offshore projection of Viveiro Fault
W
CIZ and GTMZ
WALZ
E
Variscan thrusts reactivated as late Variscan extensional detachments
Variscan thrust faults
Extended and folded or boudinaged lower crust
CZ underthrusted lower crust
TWT (s)
ESCIN-3.2
ESCIN-3.3
35 km
WALZ
CZ
Rooting of the CZ sole thrust into the hinterland
CZ sole thrust
Alpine lower crustal imbrication (E-W image of the N-S thickenning observed in Fig. 4)
ESCIN-1
b
SW
SPZ
AC
OMZ
CU
CIZ
NE
Variscan thrust faults
IRB emplaced in mid-crustal discontinuity
Variscan structures affecting pre-Variscan laminated lower crust
Pre-Variscan laminated lower crust
Crocodile-like structure: shortening in the lower crust
IBERSEIS
35 km
Onset of late-Variscan extensional tectonics: crustal thinning and melting
Vertical vertical folds: little shortening and transparent upper crust
Granites, migmatites and normal faults
Crocodile-like structure: shortening in the lower crust
Pre-Variscan laminated lower crust
ALCUDIA
35 km
Main lithological boundaries
Internal reflectivity
Interpreted fault motion
Small scale evidences of extension
Extensional detachments
Mid-crustal discontinuity and IRB
Moho
Mesozoic and Cenozoic sediments
Upper crust
Lower crust
ICS granites
Granites and metasediments?
c
Elevation (km)
TB
ICS
DB
SSE
NNW
Newly defined discontinuity after crustal melting affects the Iberian Massif mid-crustal discontinuity
Distance (km)
CIMDEF

Figure 9

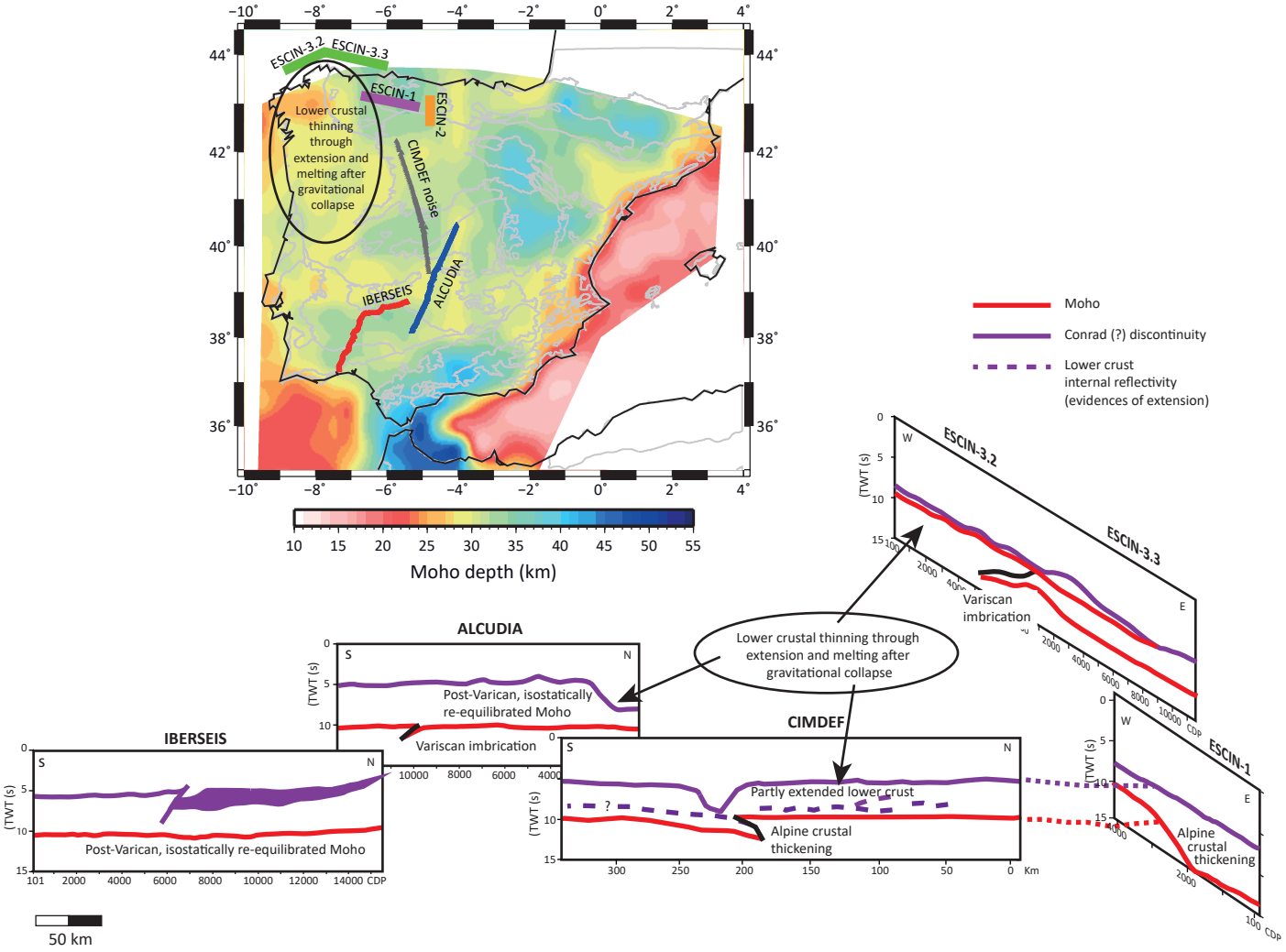
ESCIN-3.2
ESCIN-3.3
ESCIN-1
ESCIN-2
CIMDEF noise
ALCUDIA
IBERSEIS
Lower crustal thinning through extension and melting after gravitational collapse
Moho depth (km)
Moho
Conrad (?) discontinuity
Lower crust internal reflectivity (evidences of extension)
Variscan imbrication
Post-Varican, isostatically re-equilibrated Moho
Partly extended lower crust
Alpine crustal thickening
50 km

Figure 10